IOPscience iopscience.iop.org

Home Search Collections Journals About Contact us My IOPscience

Alligator clips to molecular dimensions

This article has been downloaded from IOPscience. Please scroll down to see the full text article.

2008 J. Phys.: Condens. Matter 20 374116

(http://iopscience.iop.org/0953-8984/20/37/374116)

View the table of contents for this issue, or go to the journal homepage for more

Download details:
IP Address: 129.252.86.83
The article was downloaded on 29/05/2010 at 15:05

Please note that terms and conditions apply.

J. Phys.: Condens. Matter **20** (2008) 374116 (21pp) doi:10.1088/0953-8984/20/37/374116

Alligator clips to molecular dimensions

Nicholas Prokopuk[1] **and Kyung-Ah Son**[2]

[1] NAVAIR Research Department, Chemistry Branch, China Lake, CA 93555-6100, USA
[2] Jet Propulsion Laboratory, Pasadena, CA 91109, USA

Received 13 May 2008
Published 26 August 2008
Online at stacks.iop.org/JPhysCM/20/374116

Abstract

Techniques for fabricating nanospaced electrodes suitable for studying electron tunneling through metal–molecule–metal junctions are described. In one approach, top contacts are deposited/placed on a self-assembled monolayer or Langmuir–Blodgett film resting on a conducting substrate, the bottom contact. The molecular component serves as a permanent spacer that controls and limits the electrode separations. The top contact can be a thermally deposited metal film, liquid mercury drop, scanning probe tip, metallic wire or particle. Introduction of the top contact can greatly affect the electrical conductance of the intervening molecular film by chemical reaction, exerting pressure, or simply migrating through the organic layer. Alternatively, vacant nanogaps can be fabricated and the molecular component subsequently inserted. Strategies for constructing vacant nanogaps include mechanical break junction, electromigration, shadow mask lithography, focused ion beam deposition, chemical and electrochemical plating techniques, electron-beam lithography, and molecular and atomic rulers. The size of the nanogaps must be small enough to allow the molecule to connect both leads and large enough to keep the molecules in a relaxed and undistorted state. A significant advantage of using vacant nanogaps in the construction of metal–molecule–metal devices is that the junction can be characterized with and without the molecule in place. Any electrical artifacts introduced by the electrode fabrication process are more easily deconvoluted from the intrinsic properties of the molecule.

(Some figures in this article are in colour only in the electronic version)

1. Introduction

As electronic circuits approach sub 50 nm dimensions, the size constraints, fabrication cost, and physics of conventional silicon chips face severe technological challenges [1]. Consequently, new materials with the desired electronic properties and functionality are being pursued to construct memory devices and logic circuits with dimensions on the order of a few nanometers. Since Aviram and Ratner first postulated that the electronic properties of a molecular dipole can mimic that of a diode [2], the field of molecular electronics was born and the prospects of constructing transistors, switches, and resistors from molecules promised an alternative to silicon based technologies with nanometer-sized components [3, 4]. However, interfacing the molecular nanostructures into integrated circuits requires controlled placement of electrical contacts with subnanometer resolution. Reliably configuring metal electrodes with the necessary separations capable of linking nanometer-sized component remains a major obstacle to generating molecular circuits.

In order to simply compare the electrical properties of a saturated alkyl chain and a conjugated oligo(phenylene vinylene), the organic molecules must be connected between electrical leads that interface the macroscopic dimensions. More complex circuits comprising hundreds or thousands of molecular switches with the necessary interconnections between the nanodevices and external connections to input and output leads pose even greater challenges to the field of molecular electronics. Reed and Tour [5] demonstrated one of the first experimental measurements of a molecule's conductivity by constructing metal–molecule–metal junctions from a mechanical break in a gold wire. Although the mechanical break junctions are not easily incorporated into more complex circuitry, they demonstrated that metal electrodes could be generated with the nanometer separations necessary to bridge molecular circuits to macroscopic leads. Subsequently, several approaches to generating metal–molecule–metal devices have been developed for probing the electronic properties of organic elements and constructing arrays of molecular junctions in complex circuits.

Careful manipulation and fabrication of metal electrodes with well-defined separations that are on the order of a few nanometers is possible with varying degrees of complexity.

 © 2008 IOP Publishing Ltd Printed in the UK

Nanojunctions have been formed using electromigration techniques [6], electrochemistry [7], nanolithography [8], scanning probes [9], break junctions [5], and crossed wires [10]. Levels of sophistication range from the surprisingly simple mercury drop contacts [11] that utilize nothing more than ordinary lab equipment to make a top contact to a self-assembled monolayer (SAM) on a metal film to more intricate scanning probe and electron-beam lithographic techniques that require dedicated instrumentation worth hundreds of thousands or millions of dollars [12]. Despite these great differences, the various strategies for generating metal–molecule–metal junctions can be categorized into two basic approaches. In the first, a top-contact is made to a molecular film deposited on a conducting substrate. The second strategy involves fabricating vacant nanogaps and subsequently inserting a molecular element between the nanospaced electrodes. There are a number of variations within the two approaches and each unique process for connecting a molecule between two electrodes entails its own set of advantages and disadvantages. The goal of this review is to highlight the different approaches for constructing nanojunctions suitable for studying electron tunneling in metal–molecule–metal devices.

2. Top-contact junctions

In the top-contact method, a SAM or Langmuir–Blodgett (LB) film containing the specific molecular component with the desired electrical properties is initially deposited on a conducting substrate. The interface between the substrate and SAM or LB film serves as one metal–molecule connection (bottom contact). A top contact is then made to the top or exposed surface of the organic film. The two contacts connect the molecules in the SAM or LB film to external circuits. Several strategies for making the top contact have been reported including conventional scanning probes [9], thermally deposited metal layers [13], mercury drops [11], metal colloids [14], and crossed-wire junctions [10]. The key advantage of the top-contact approach is that the SAM and LB films containing the molecular component sets the electrode spacings at the precise distance needed to connect the two ends of the molecule. In effect the molecular element acts as both circuit element and template for controlling the metal–metal separation. Top-contact metal–molecule–metal connections are possible regardless of the molecule's length or thickness as long as the molecule is within a stable and robust SAM or LB film that prevents shorting when the top contact is added. One benefit of employing the top-contact method is that asymmetric molecules can be uniformly aligned normal to the surface to investigate the directional tunneling properties of a molecular dipole. The flexibility in the types of molecules that can be assembled into SAMs and LB films, control over their orientation within the film, and the straightforward methods for adding a top contact make the top-contact approach extremely versatile for investigating charge transport through a diverse range of structures.

The length of metal–molecule–metal junctions constructed from the top-contact method is typically on the order of a single-molecule layer or bilayer. However, the cross-sectional area of the metal leads are typically much larger than the footprint of a single molecule. Consequently, the process used to establish the top contact dictates the overall dimensions of the device. Lithographically patterned top contacts are convenient for constructing large integrated arrays of molecular circuits with cross-sectional areas that are significantly larger than the dimensions of the molecular elements. By contrast, scanning probes on SAMs can reduce the footprint of the molecular junction to a single molecule. However, probe techniques are ill suited for constructing integrated circuits comprising hundreds or thousands of devices. Metal–molecule–metal devices constructed with large top contacts contain multiple molecules in parallel within each junction. Significant differences between the collective properties of these ensembles and the tunneling properties of a single-molecule junction can contribute to unexpected conductance values. As a result, the normalized conductance of molecular resistors varies with the size and type of the top contact [15]. Moreover, devices with large footprints greatly increase the dimension of the circuit element beyond the few square nanometers promised by a single-molecule transistor.

Importantly, the method used to establish the top contact can have a dramatic effect on the organic layer and introduce electrical artifacts that are difficult to differentiate from the intrinsic properties of the molecule. The absence of obvious control experiments, such as obtaining the electric response of the junction in the absence of the molecule or measuring the molecule's conductance without the metal contacts, further convolutes the resistivity of the molecule with the effects of the top contact. Once the top contact is in place, the spectroscopic tools available for characterizing the intervening molecule are greatly limited by the metallic properties of the metal electrodes which prevent the transmission of vibrational spectra. Inelastic tunneling spectroscopy can provide low-temperature structural information on the molecular junction [16]. Knowledge of the structure and function relationship of the organic film is important in identifying the mechanisms responsible for switching a molecule's resistance between conducting and nonconducting states. This is all the more important if the electronic properties of the metal–molecule–metal junction are to be controlled by chemical changes in the molecular component.

2.1. Scanning probes

Scanning tunneling microscopy (STM) provided some of the earliest attempts to connect macroscopic leads to molecular circuits [17, 18]. STM and the more recently developed technique of conducting atomic force microscopy (c-AFM) operate on similar principles: a metallic tip is brought into close proximity to a conducting substrate and a bias is placed between the tip and substrate [19]. Current flowing between the tip and surface is used to quantify the resistivity of molecules immobilized on the substrate. The advent of scanning tunneling spectroscopy (STS), which monitors the change in current as a function of potential, allowed resistivity data of a molecular film to be obtained with subnanometer spatial resolution [20]. One of the early uses of STS

on self-assembled monolayers adsorbed to gold substrates demonstrated the rectification behavior of easily polarized oligo(phenylene ethynylene) structure and, thus, confirmed Aviram and Ratner's prediction [21].

The spatial resolution of the scanning probes is well suited for accessing arrays of molecular on/off switches for memory storage. In this application, a molecular memory unit is toggled between high and low conductive states with a unipolar pulse. Individual molecules with cross-sectional areas of a few nanometers are easily distinguished from an insulating background [22]. Thus, the memory unit is reduced to the dimensions of the molecular element and the insulating (nonconducting) surrounding. Unfortunately, metal–molecule–metal junctions formed with top contacts made with a scanning probe lack the interconnectivity necessary for logic operations and are not readily adaptable for working collectively in tandem due to the piezoelectric translational mechanism used to move the contacting tips.

In conventional STM experiments on SAMs bound to gold surfaces, the metal tip is separated by some distance from the molecular layer. A tunneling current flows via overlap of the wavefunctions of the tip and molecule with an applied bias. The tip–molecule distance can fluctuate over the timescale of the STS or STM experiment. Due to the exponential dependence of the tunneling current on distance, a small deflection in the tip height significantly affects the electric current. However, over shorter time periods, the tip–molecule separation can be considered constant allowing I–V measurements on a relatively static metal–molecule–metal junction. The presence of a gap between the tip and molecule introduces an additional resistive element that must be deconvoluted from the electrical measurements in order to extract the molecule's conductance [23]. Mechanical contact between the tip and molecule can minimize the top contact-molecule resistance. However, care must be taken to limit tip-induced deformations in the molecular film such as bends or conformational changes which can dramatically affect the tunneling resistances by several orders of magnitude [24, 25].

With a combination of current–voltage and current–distance measurements, c-AFM, STM and STS can yield relative barrier heights [26–28], negative differential resistance [29, 30], phase differences [31], stochastic conductivity switching [22, 32, 33], redox-activated switching [34], photo-induced resonant tunneling [35], supramolecular coupling [36], and conformational changes [37, 38] in a variety of molecular structures self-assembled on gold surfaces. In one set of experiments, Tour's group utilized a 10 kHz data collection with a fixed lateral position to monitor the conductivity of oligo(phenylene ethynylene) and related molecules as a function of time [32, 33, 37, 38]. Surprisingly, they found that the apparent height of the oligomers varied stochastically between two values under constant current conditions, figure 1. These observations were ascribed to changes in the electronic structure of the oligomer–metal interactions resulting from oscillations in the molecule's binding to the surface. As the molecule fluctuates between two binding modes, the barrier height of the junction changes resulting in apparent increases or decreases in height (on/off states). Furthermore, Tour's group was able

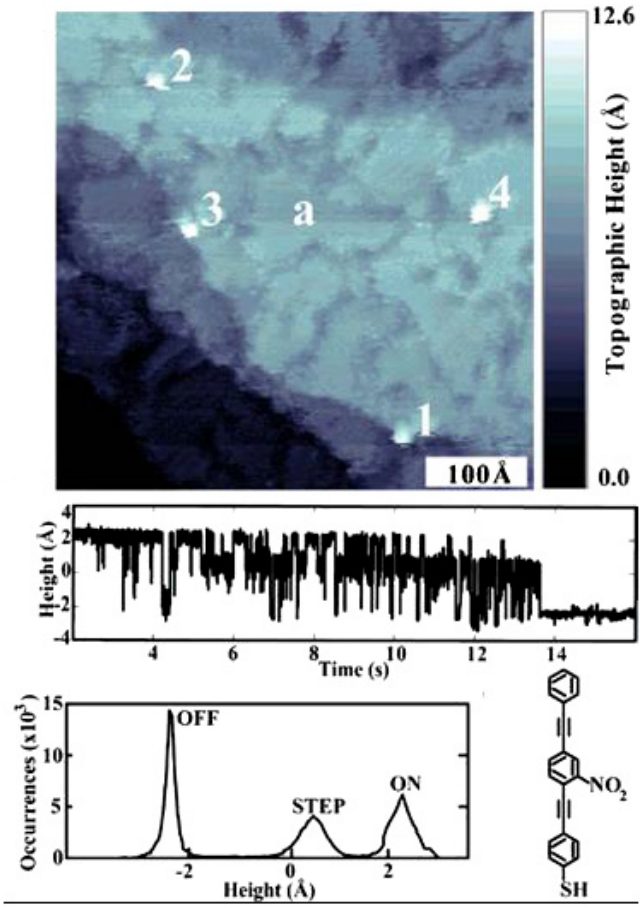

Figure 1. STM topological map of a gold surface (top) modified with the nitro-oligo(phenylene ethynylene) in a host dodecanethiol monolayer. The real-time height versus time plot (middle) indicates a switching of the height of the oligomer. The occurrence versus height plot (bottom) indicates ON, OFF, and STEP states [32]. Reprinted with permission from [32]. Copyright 2007 American Chemical Society.

to control the preferred conformation by altering the chemical environment surrounding the oligomer [33]. Insights into a molecule's electrical properties can still be acquired with conventional scanning probe microscopy and spectroscopy despite the presence of a gap resistance between the probe tip and molecular element.

The distance between the probe tip and the molecular film can be effectively reduced to zero by forming a covalent attachment between the SAM and the metal tip. In this approach a symmetric bisthiol such as 1,6-hexanedithiol extends from a gold substrate to a c-AFM or STM tip. The distill thiol attaches to the tip creating a covalent metal–molecule–metal junctions which lacks the gap resistance between the top of the SAM and the probe tip. With the symmetric linkage, the metal–molecule interfacial resistances are more easily identified from the current–distance profiles [39]. However, in this close proximity to the surface, the probe tip is susceptible to covalent attachment to multiple molecules within the SAM layer. Single-molecule conductivities can be obtained by pulling the probe tip away from the surface and systematically breaking the covalent linkages to the thiols [9, 25, 40–43]. As each organothiol

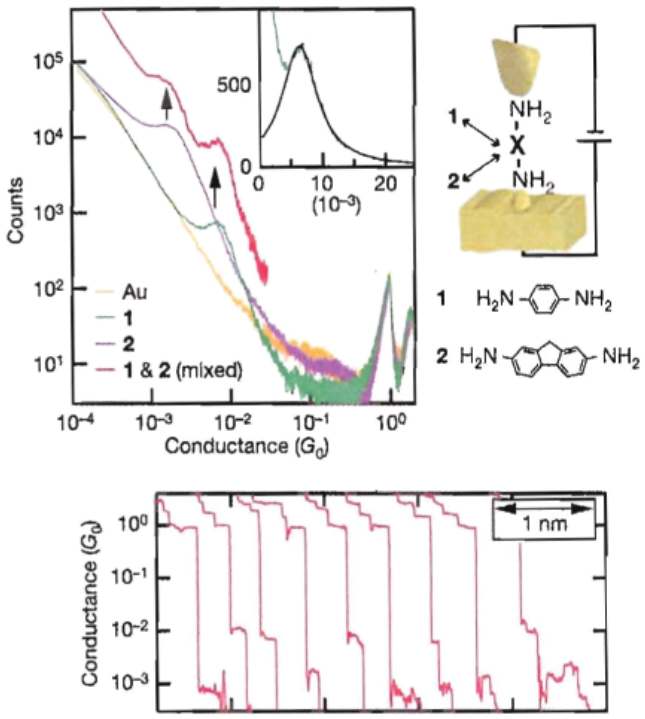

Figure 2. Histogram of conductance values (top left) obtained from metal–molecule–metal junctions formed with scanning probes on SAMs of 1,4-diaminobenzene (1) and 2,7-diaminofluorene (2) and conductance traces obtained by raising the probe tip away from the surface [9]. Reproduced with permission from [9]. Copyright 2006 Wiley-VCH Verlag GmbH & Co.

disconnects from the surface or the tip, a covalent pathway for electron tunneling is broken and the conductivity of the junction drops. Since each thiol provides nearly the same resistance, the drop in current is stepwise and each drop in conductance corresponds to that of a single bridging bisthiol. By repeatedly forming and breaking contact between the probe tip and the surface-bound molecule, histograms of the organic film's conductance can be obtained with peak values, figure 2. It should be noted that each drop in current is not in perfect unity since the resistance of individual molecules changes as the organothiol's geometry deforms during the stretching process. Interestingly, just prior to breaking a metal-thiol connection, the conductance of the bridging alkyl chain increases. This small improvement in the alkyl's resistance is attributed to changes in the confirmation of the chain from *gauche* to the all-*trans* configuration [42]. Kushmerick and Bazan compared the conductivities of thiol-terminated oligo(phenylene vinylene)s obtained with conventional STM and contact-AFM [44]. In these experiments the coordination of a single thiol to the gold surface in the asymmetric junctions of a non-contacted STM splits the low-lying molecular orbitals of one half of the organic fragment. In contrast the symmetric metal–molecule–metal junction formed with the c-AFM and the bisthiols results in an even distribution of the molecular orbitals through the entire molecule and a higher conductance. The perturbation of the molecule's orbitals by the sulfur's bonding to the surface suggests that the linking mechanism between the molecular circuits and the electrical leads can greatly influence the device performance.

2.2. Permanent top contacts

Integrated circuits of metal–molecule–metal junctions require robust electrode geometries that can be deposited or printed over large areas. Thermal deposition or contact printing of a top electrode on a SAM or LB film yields physically stable molecular circuits using simple lithography to pattern the electrodes. Top contacts in metal–molecule–metal junctions formed from deposited metal layers are not easily removed without destroying the circuit. While the size of these devices is not significantly improved over silicon based circuits, they demonstrate that molecular elements can be incorporated into working circuits that interface with external electronics. A significant benefit of these permanent top-contact junctions is that the lithography used to pattern the metal electrodes can also construct interconnects that join the molecular junctions to each other and to external circuits on macroscopic dimensions. For example, crossbar networks formed from orthogonal arrays of metal wires sandwiching molecular switches have been prepared and successfully demonstrated logic functions and memory storage [45, 46]. Junctions composed of 40 nm wide wires and cross-sectional areas of 1600 nm^2 containing approximately 1100 molecules each [47]. Crossbar arrays have been prepared with device yields of 85% and a nonvolatile memory density of 6.4 Gb cm^{-2}. While the mechanism responsible for conductivity switching in these circuits is uncertain, the lithographically produced architectures demonstrate that functional electronics can be constructed from metal–molecule–metal circuits on a large scale.

A significant portion of the work on metal–molecule–metal junctions with permanent top contacts has been performed using thermally deposited metal leads. Studies on the interactions of organic SAMs and LB films and metal vapor such as that from thermally deposited titanium/gold contacts indicate that the metal–molecule interface is not necessarily discrete. Specifically, interfacial reactions between the depositing metal film and the organic layer can introduce new chemical species with unknown electronic states. For example, titanium patterned on alkyl layers results in metal carbide formation [48, 49]. By contrast naphthalenes remain undamaged after titanium deposition keeping the molecule's electronic properties intact [50]. Extensive studies on the effect of the head group of the organic film on the reactivity of the SAM with vapor phase metal reveal that monolayer degradation can occur by several different mechanisms [51, 52]. The electronic properties of metal carbides within the gaps can dominate the energetics and charge transport properties of the metal–molecule–metal junctions and override any contributions of the molecular complex. Importantly, the integrity of the organic film should not be assumed to remain intact as the deposition of the top contacts may introduce electronic artifacts into the nanogap and alter the chemical composition of the junction.

Despite complications arising from chemical reactions between the metal leads and the organic film, viable circuits have been fabricated with thermally deposited top contacts on redox active films of rotaxanes and catenanes. Metal–molecule–metal junctions composed of these supramolecular

complexes sandwiched between thermally deposited gold electrodes exhibit large hysteresis in their I–V curves [45, 46]. The conducting and nonconducting states of the rotaxanes and catenane are sufficiently different that they can be assigned binary values. The unipolar voltage-switching of the junction's resistance was initially attributed to changes in the oxidation state of the molecules and any concomitant structural changes caused by the redox process. Subsequent studies on thermally deposited top-contact metal–molecule–metal devices revealed that the conductance switching is independent of the type of molecule in the junction. For example, metal–molecule–metal junctions fabricated from LB films of fatty acids exhibit similar conductance switching properties as those constructed with the more complex rotaxane molecules despite lacking the redox activity of the rotaxanes [53]. Consequently, the mechanism for effectively toggling the resistivity of the rotaxane and alkyl chain is most likely not molecular in nature. Rather, metal ion motion from the metal electrodes and filament formation likely play a more significant role in determining the electronic properties and conductivity switching in these junctions with thermally deposited top contacts [54–58]. Both phenomenons can result in the unipolar switching behavior observed in the fatty acid and rotaxane films. While these devices demonstrate practical control over the conductance of a molecular circuit for memory and logic operations, the nonmolecular explanations of the switching mechanism suggest that the molecular properties of the junctions are not being fully utilized. Fine tuning of the chemical component in these junctions is unlikely to produce rational improvements in device performance. More gentle means for making the top contact such as contact printing of the metal electrodes can also result in unexplained hysteresis effects [59]. A more thorough understanding of the metal–molecule interfaces is needed before conclusions about the molecule's electronic properties and switching mechanism can be made from thermally deposited top contacts. Additionally, concerns with filament formation and metal ion migration may not be limited to thermally deposited and printed top-contact devices and are potentially a problem for other nanometer-sized junctions operating under similar temperatures and current densities.

Perhaps more problematic for metal–molecule–metal junctions formed with thermally deposited top contacts is evidence that the metal vapor can penetrate the SAMs and react with the underlying substrate [52, 60, 61]. Compromises in the integrity of the organic film can lead to significant deviations from the discrete metal–molecule–metal model as the metal vapor pushes into the molecular layer and provides an alternative, or nonmolecular, pathway for electron transfer. Interestingly, the penetration depth of the metal vapor not only depends on the organic film but also on the composition of the underlying substrate material and its effect on the integrity of the LB film. Cadmium stearate LB films formed on gold decompose when exposed to titanium vapor [62]. By contrast, the same LB film on platinum oxide surfaces remains intact after titanium deposition. The sensitivity of the organic films to metal vapor requires that care must be taken to ensure that the molecular elements form a robust film capable of preventing metal atoms from penetrating to and reacting with the underlying substrate. The cross section of the molecular junctions and the available area for metal vapor to penetrate can be reduced with a nanopore to house the organic SAM [63–65]. This strategy reduces both the size of the molecular junction and the possibility of deleterious interactions between the metal vapor and organic phase.

Metal–molecule–metal junctions fabricated with the top-contact method require the effects of the top contact to be considered when interpreting the electrical response of the device. Despite the successful construction of integrated circuits that demonstrate logic functions using molecular switches and thermally deposited or printed leads, the structure and function of the molecular component and its role in the conductance switching mechanism is not clear. By employing different methods for introducing the top contact, the conductivity of molecular resistors can be studied in a variety of configurations and testbeds. A combination of scanning probes, crossed-wire junctions, and metal bead contacts with a series of alkyl chain, oligo(phenylene ethynylene)s, and oligo(phenylene vinylene)s reveal the same trend in conductance regardless of the technique [66]. Similar multi-prong approaches can more readily identify gross effects of a top contact in any one testbed and help isolate the electrical properties that are intrinsic to the molecule.

2.3. Crossed-wire junctions

Crossed-wire junctions are a unique approach to fabricating metal–molecule–metal circuitry. Crossed-wire tunneling junctions form when two orthogonal gold wires (10 μm diameter) approach each other within tunneling distance. One of the wires is chemically modified with a SAM [10]. The wires are brought close to each other by a Lorentz force between the dc current in one wire and an external magnetic field. The Lorentz force deflects the wire eventually reducing the separation between them. When the wires come into contact, a tunneling junction is formed with the gold wires acting as leads. The interwire current passes through the SAM providing information on the electrical properties of the organic layer, figure 3. The diameter of the gold wires determines the cross-sectional area. Thinner wires produce junctions containing fewer molecules and more narrow tunneling pathways. Since the wire diameters are large compared to the molecule's footprint, collective properties of the molecular ensemble contribute to the junction's conductance. As expected, the interwire currents were found to be highly dependent on the electronic structure of the organic molecules with oligo(phenylene vinylene) monolayers yielding interwire currents that are several orders of magnitude larger than the more insulating alkyl chains [10]. These results are qualitatively consistent with molecular conductivities obtained with other testbeds including STM and metal bead contacts [66].

The crossed-wire experiments are ideal for studying subtle effects such as the importance of pressure exerted by the top contact on the conductance of molecular resistors in a metal–molecule–metal junction. Since the top contacts rest on the molecular layer, the force exerted normal to the

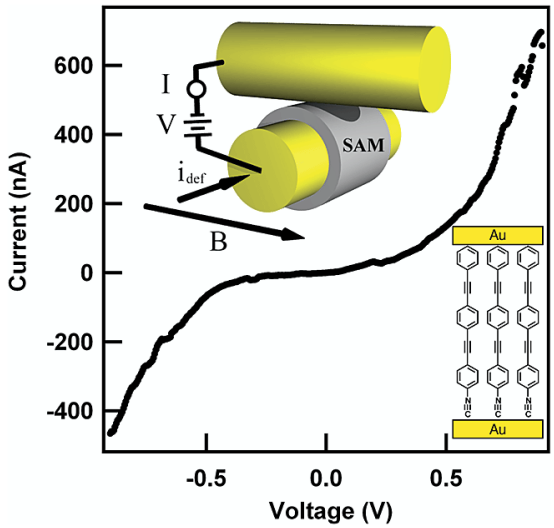

Figure 3. *I–V* properties of a metal–molecule–metal junction formed by crossed wires with oligo(phenylene ethynylene)s [156]. Reprinted with permission from [156]. Copyright 2004 American Chemical Society.

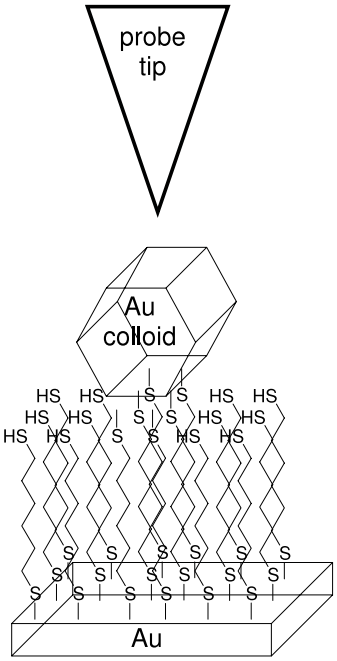

Figure 4. Schematic of a gold cluster top-contact junction.

molecular film can lead to physical deformation in the bridging molecules. The molecular component responds to the force of the top contact through a simple conformational change in the molecule's geometry or a contraction of the molecule's bonds and angles. Physical changes in the geometry of the molecule readily affect the molecule's electronic structure and conductance compared to a stress-free junction [24, 25]. In a crossed-wire junction, the load between the wires can be changed by increasing or decreasing the Lorentz force. With increasing pressure the conductance of oligo(phenylene vinylene)s increase by a factor of 100 beyond what is expected for a simple change in the contact area [10]. Presumably, deformations of the SAM layer results in a compression or stretching of the molecular elements and a change in the HOMO and LUMO energies and the molecule's barrier height. Additionally, the formation of alternative (through space) pathways cannot be ruled out in these compressed systems. A similar pressure dependence is observed for c-AFM measurements on SAMs of alkanethiols at high force conditions [67]. In metal–molecule–metal junctions with more static configurations such as the top contacts formed by the thermal deposition of a metal layer on a LB film, subtle pressure effects can still contribute to the variability in the configuration and tunneling properties of the organic component. Consequently, the measured resistance of molecular wires varies depending on the specific experimental conditions used to connect the molecule to electrical leads. For example, scanning probe measurements (c-AFM and STM) and Hg-drop experiments on monolayers of alkyl bis and monothiols result in molecular conductivities that vary by several orders of magnitude for alkyl chains of similar length [68].

2.4. Metal beads

Metal beads or colloidal metal particles dispersed on a SAM provided one of the early top contacts for metal–molecule–metal junction [69]. Small gold clusters of a few nanometers in diameter can serve as electrical leads that cover relatively few molecules in the organic film compared to lithographically patterned top contacts, figure 4. To complete the metal–molecule–metal cluster circuit, the tip of a scanning probe connects to the individual metal clusters. A mechanism for anchoring the metal beads to the SAM such as covalently attaching the particles to the organic film is employed to limit lateral motion of the metal particles. For gold clusters, monolayers composed of symmetrically terminated bisthiols provide a distal thiol group disposed away from the surface that is available to bind the metal cluster [15, 69]. The number of molecular elements that bridge the conducting substrate and the metal particle can be further reduced by diluting the bisthiols in a monolayer composed primarily of monothiols which lack the secondary thiol needed to attach to the metal bead [15]. The conductance of metal–molecule–metal cluster junctions constructed with carotenes dispersed in highly resistive docosanthiol films are integer multiples of a parent conductance that is assigned to that of a single carotene [15]. Resistance between the probe tip and the metal particle can lead to charging or Coulomb blockade events which manifest in the *I–V* properties of the junction and require deconvolution from the inherent properties of the molecular component. Larger gold particles (>5 nm) can reduce both the tip bead resistance and Coulomb charging barriers [70]. Unlike the break junctions formed by direct contact between the scanning probes and bisthiols in a monolayer or the crossed-wire platform, the conductance values of molecular junctions formed with metal beads are not as strongly dependent on the force exerted by the contacting probe used to connect the metal cluster to the external circuit.

Integrated circuits constructed from metal bead top contacts require that the clusters assemble in an organized and controlled fashion. Monolayers of pure bisthiols

Figure 5. Micrograph of a magnetic bead bridging two $Ni_{80}Fe_{20}$ electrodes. The scale bar is 1 μm [14]. Reused with permission from [14]. Copyright 2005, American Institute of Physics.

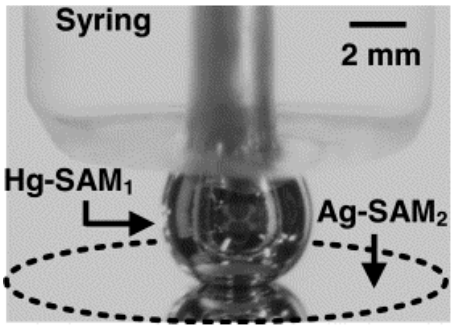

Figure 6. Photograph of a mercury top contact on a SAM-coated silver surface [78]. Reprinted with permission from [78]. Copyright 2002 Elsevier.

serve as sticking boards to gold clusters without providing any means to limit or manage the placement of the top contacts. Bisthiols dispersed in monothiol layers limit the gold cluster deposition only to the sites where the bisthiols are located [70]. However, selecting the placement of the bisthiols within a film of monothiols poses it's own challenges. Kushmerick demonstrated the directed assembly of metal colloid top contacts with magnetic particles made by sequentially coating silica microspheres with nickel and gold [14]. The ferromagnetic nickel layer contributes a magnetic moment which provides a mechanism for controlling the placement and orientation of the particle. The Au/Ni particles undergo directed assembly on arrays of magnetic electrodes coated with SAMs, figure 5. In this geometry, the metal beads span two electrodes coated with a SAM and two metal–molecule–metal junctions are formed in series. Parsons used dielectrophoresis to trap nanoparticle–molecule–nanoparticle dimers between electrodes [71]. The gold nanoparticle dimers exhibit stable I–V properties with bridged oligomeric phenylenes. Electrostatic trapping of single gold nanoparticles between metal electrodes separated by tens of nanometers [72] and coated with organic monolayers also forms stable metal–molecule–colloid–molecule–metal bijunctions [73, 74]. Directing large numbers of metal particles between patterned electrodes promises a straightforward, if cumbersome, method for generating arrays of molecular junctions.

2.5. Mercury drops

While neither structurally robust nor easily integrated into micro-or nano-sized circuits, liquid mercury contacts to molecular resistors and switching elements provide a simple and low-cost method for studying metal–molecule–metal junctions. Mercury contacts to molecular circuits were first reported by Whitesides [75] with SAMs of organothiols or disulfides separating two mercury drops. The initial work focused on the alkyl layers as nanoscale dielectrics in capacitors [11, 75]. In these experiments, the liquid mercury surfaces provide smooth and defect-free platforms for SAMs of organosulfur compounds coating the two Hg-droplets. Electrical measurements across the SAM-coated mercury drops yield conductance values for the organic bilayer separating the liquid metal including the resistivity of the noncontacting gap between the SAM layers [76].

Subsequent work [77–81] with mercury top contacts demonstrated that liquid leads can be employed with solid silver and gold bottom contacts with organic thiols and disulfide monolayers, figure 6. In these devices the morphology of the solid metal electrode greatly influences the conductance of the junction [81]. The interface of highly crystalline silver films in a mercury-bilayer-silver device yields more reproducible I–V behavior with a narrower current density distribution than interfaces formed with less crystalline silver. Unlike the mercury-bilayer-mercury junctions that contain SAMs of the same molecule on each metal surface, junctions with mercury and a solid metal contact can be constructed with dissimilar SAMs on the two leads allowing for asymmetric bimolecular circuits. Rectification in tunneling currents between mercury-bilayer-silver (and gold) was observed with bilayers composed of two different SAMs, one containing a tetracyanoquinyl group and the second an n-alkyl chain [79]. Bilayers composed of alkyl chains of two different lengths also exhibit rectification [80]. Interestingly, a single layer of alkyl thiolate between two mercury drops produce symmetric I–V curves indicating no rectification despite the two different metal–molecule interfaces (covalent Hg–S and noncovalent Hg$\cdots$$CH_3$–) [82]. The resistance of the single-molecule junction is an order of magnitude greater than that obtained for bilayers containing the same number of carbon atoms indicating that the nonbonding methyl–mercury junction is significantly more resistive than the methyl–methyl interface of a Hg-bilayer-Hg device.

While mercury top contacts are unlikely to find applications in the construction of integrated circuits, a number of metal–molecule–metal junctions generated with liquid mercury top contacts have produced particularly significant results for molecular and solid-state electronics. In one set of experiments [83, 84], the conductance of electroactive bilayer films of $(NH_3)_5$Ru(pyridyl) sandwiched between mercury drops was observed to change by several orders of magnitude upon oxidation of the Ru-centers with a three-electrode configuration, figure 7. The oxidation potential of the Ru-centers within the junction is not significantly shifted from that of the molecule dispersed in solution suggesting that changes in the Ru-centers' electronic structures are responsible for the conductance increase. Mercury top contacts have

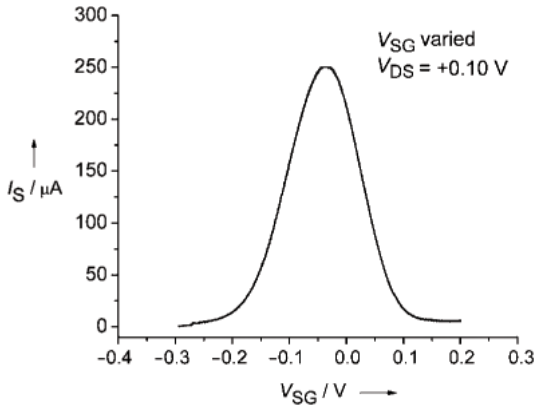

Figure 7. Transistor-like behavior of a Hg-(pyridyl)Ru$(NH_3)_5^{2+}$(NH$_3$)$_5$Ru(pyridyl)Hg junction [83]. Reproduced with permission from [83]. Copyright 2004, John Wiley & Sons, Inc.

also been used to investigate Schottky diodes at Hg-molecule-semiconductor junctions [85]. Diodes formed from mercury drops on silicon surfaces that are chemically modified with insulating *n*-decyl chains exhibit near-ideal rectifying behavior that is superior to similar devices fabricated with the native silicon dioxide layer as the insulator. The excellent diode behavior and model energetics observed for the Hg-decyl-silicon junctions indicates that Hg atom migration and silicide formation are not contributing to the dynamics of the charge transfer process at these Schottky junctions. The simplicity of forming liquid mercury top contacts provides a simple route to metal–molecule–metal and metal–molecule-semiconductor junctions with few electrical artifacts resulting from the introduction of the top contact.

3. Vacant nanogaps

Constructing vacant nanogaps with specific electrode geometries and separations that are suitable for molecular electronic application is somewhat more challenging than the top-contact approach. Unlike the top-contact method in which the metal contacts are built around a specific molecular element that doubles as a template for defining the metal–metal separation, fabricating vacant gaps with nanometer dimensions requires alternative strategies to control the metal–metal distance (gap sizes) with great precision. Small deviations in the electrode separations can prevent the molecular component from spanning the two electrodes. For example, biphenyl-4,4′-dithiol can effectively bridge gold electrodes that accommodate the 10.7 Å separating the sulfur atoms. A deviation of 1 Å in the metal–metal separation can prevent the molecule from covalently bridging the metal leads. Smaller gaps require the molecule to adopt a tilted orientation to fit within the available space which may provide alternative tunneling pathways or deformations in the molecule and the molecular orbitals involved in electronic coupling [25]. For molecular electronic applications, a large distribution in electrode spacings can compromise device yields as gaps that are too large or too small may result in irregular electrical properties. Thus, spatial control of the metal–metal separation is crucial for the vacant nanogaps to reliably form metal–molecule–metal junctions with consistent and predictable properties. This added challenge poses a significant hurdle to the development of vacant nanogaps in molecular electronics applications. However, within the last few years several new and promising methods have been reported for generating nanospaced electrodes with well-defined separations that are on the order of a few nanometers. Although some of these new techniques have not been specifically used to fabricate covalent metal–molecule–metal junctions, their metal–metal spacings are readily suited for studying electron tunneling across molecular dimensions.

Generating vacant nanogaps between metal electrodes requires a mechanism for controlling metal–metal separations with subnanometer precision. To control and manipulate the metal–metal distances with the necessary accuracy requires novel fabrication methods as these feature sizes are beyond the limits of conventional lithography. Two strategies are commonly employed for introducing nanogaps between metal electrodes. In one method, a feed back loop monitors *in situ* an electronic signal during the deposition or erosion of metal that ultimately forms the electrical leads. The fabrication process is immediately stopped once a predetermined resistance is obtained. For example, electrochemically plating metal atoms on lithographically patterned leads reduces the separation between the electrodes and the conductance of the junction rises when the electrodes approach the tunneling distance and the current rapidly increases. The feedback loop can be used in conjunction with a variety of techniques for depositing or removing metal in the junction fabrication. In the second method, a sacrificial layer is used to temporarily separate the two electrodes during the fabrication process. The spacer layer determines the electrode separations and is subsequently removed leaving a vacancy between the metal electrodes. In order to obtain separations of 1–3 nm, the spacer itself must be molecular or atomic in nature. Both thin atomic films and molecular layers have been used as the templating agent for generating vacant nanogaps and arrays of empty junctions. The level of control over the electrode separations and geometries varies with the specific method and materials used to form the nanogaps.

Despite the significant challenges of fabricating vacant nanogaps, the benefit of being able to characterize the molecule-free junction and compare it to the completed metal–molecule–metal device provides substantial motivation for pursuing the vacant nanogap strategy. By first characterizing the electronic properties of the pristine empty gap ‘as made’, the resistance or switching characteristics of the molecular component can be investigated with the knowledge that any changes in the gap’s resistivity are due to the molecular element. Vacant gaps with dubious electrical properties are easily identified and discarded prior to the molecular studies. Since the molecular component is inserted only after the fabrication of the metal leads is complete, complications arising from the deposition of metal vapor on the organic films are not a concern with vacant nanogaps.

A second advantage of constructing metal–molecule–metal junctions from vacant nanogaps is the accessibility of

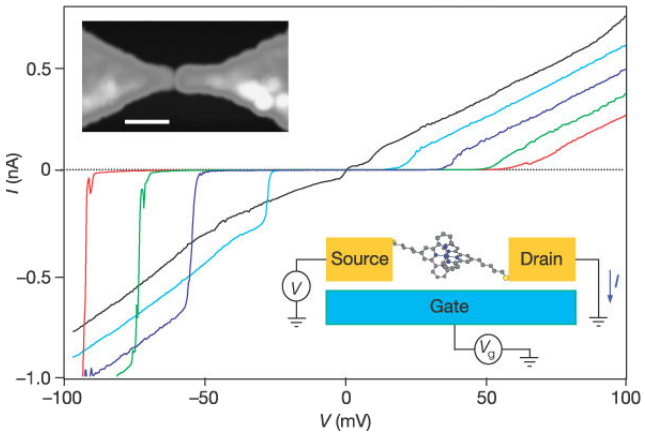

Figure 8. Three-electrode devices formed with electromigration gaps and Co-polypyridyl complexes. The topographic micrograph (top left) shows the nanogaps with a scale bar of 100 nm. The I–V curves are acquired at gate voltages raging from −0.4 V (red) to −1.0 V (black) at −0.15 V intervals [107]. Reproduced with permission from [107]. Copyright 2002 Nature Publishing Group.

horizontal electrode geometries. With coplanar electrodes, the underlying substrate can serve as a third electrical contact to the molecular component bridging two metal leads, figure 8. In these architectures, the insulating layer on the substrate serves as a dielectric separating a gate electrode from the bridging molecule. The gate toggles the electronic properties of the bridging molecule by inducing a polarizing electric field. The three-electrode configuration is similar to a conventional field effect transistor with the molecular component serving as the channel [86]. Importantly, the connection of the third electrode to the molecular circuit provides rational control over the electrical properties of the molecular channel. Mirrored charges in the electrode can serve as counter charges to the oxidized or reduced states of the molecular component. As the electronic structure of the molecule changes, the orbitals that participate in electronic coupling are altered resulting in concomitant changes in the molecule's conductivity. Care must be taken to insure that the gap between the nanospaced electrodes is free of electrical defects. Surface states on the insulating dielectric layer can contribute to the electrical response of the device. In a molecule-sized device, only a single surface defect is needed to replicate the electronic properties of a molecule dominating the conductance of a gap. By carefully characterizing the electronic properties of the vacant junction prior to introducing the organic thiols, the absence of surface states can be confirmed to ensure that the molecular element is providing the electrical response.

Nanogaps between metal leads can be fabricated using a variety of techniques including electromigration [87], electrodeposition/dissolution [88], shadow masking [89], focused ion beams [90], or selective chemical etches [91]. Once the metal electrodes are formed with the desired nanometer separations, the molecular component is subsequently inserted between the two electrodes. Importantly, the introduction of the organic element must not disrupt the electrode geometries or significantly change their composition. Organic thiols are often used to take advantage of the soft gold-sulfur affinity and generate covalent gold–molecule–gold contacts. The molecular element is often a symmetric bisthiol with the two sulfur groups disposed at opposite ends of the molecule. This geometry allows the molecule to spontaneously bridge the metal–metal gap. One disadvantage of inserting the molecular component into a premade nanogap is that asymmetric molecules will randomly orient within the junctions instead of aligning their dipoles in parallel. More sophisticated methods are required to spontaneously align the molecule dipoles such as the use of an electric field between the electrodes during the self-assembly process. Also, exposing the entire circuit to an organothiol solution will coat all exposed gold surfaces with the thiol. To some extent, thiolate coverage can be electrochemically deposited on specific electrodes [92]. Specific strategies for generating the vacant nanogaps are discussed in more detail.

3.1. Mechanical break junctions

One of the first experiments to directly probe the electronic properties of a metal–molecule–metal junction employed a mechanically-induced break in a gold wire as the nanogap [5]. In these mechanical break junctions, a metal wire is deposited on a flexible isolation substrate which rest on a piezoelectric fulcrum. The piezoelectric rod pushes upward and bends the flexible substrate fracturing the wire, figure 9. The size of the gap in the broken wire can be controlled with subpicometer resolution by varying the force of the piezoelectric rod [93]. In the initial experiments, the break in a gold wire was introduce with the wire immersed in a solution of benzene-1,4-dithiol which bridged the nanogap forming covalent linkages to the electrodes [5]. The molecular resistance in these experiments exhibited stepwise jumps of approximately 9 MΩ as the gap size was increased suggesting that this was the inherent resistance of a single benzene-1,4-dithiol. Subsequent research has employed mechanical break junctions to measure the relative conductance of a variety of molecular structures [94, 95]. Since the cross-sectional area of the break junctions are not well characterized, the number of molecules bridging these nanogaps can only be estimated in order to yield normalized conductances for the connecting molecules. By expanding the gap and breaking contact with the molecular bridges, stepwise changes in the junction's conductance reflect the electrical properties of the molecular components similar to the top-contact experiments with scanning probe break junctions. The mechanical break junctions are poorly suited for building extended arrays of molecular circuits due to the inherent size of the piezoelectric mechanism. Riel has successfully demonstrated the mechanical break junctions as platforms for unipolar switches composed of oligo(phenylene ethynylene)s [93]. Unless the piezoelectric components are significantly reduced in size, the mechanical break junctions are unlikely to find more significant applications towards constructing integrated circuits of molecular electronics.

3.2. Electromigration

Electromigration has been viewed for much of the last 100 years as a detriment to integrated circuits and a source of

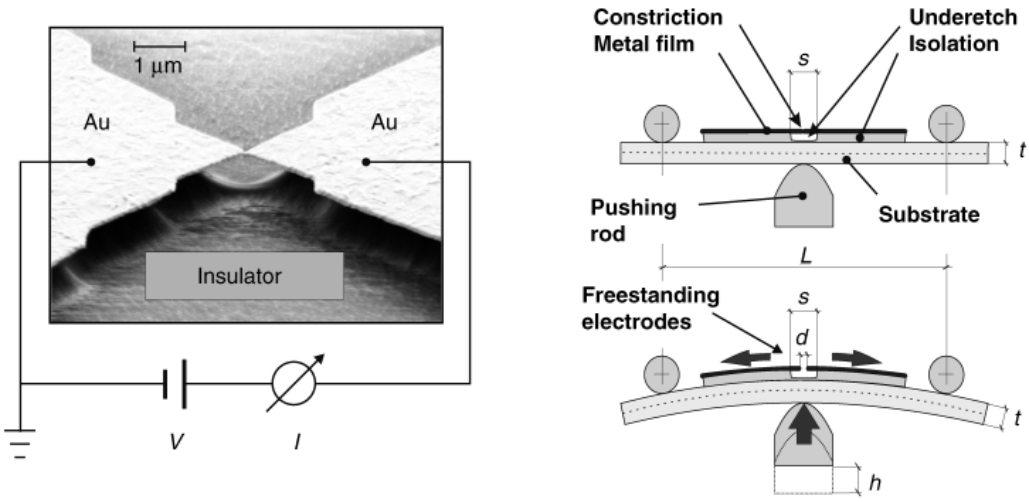

Figure 9. SEM image of a mechanical break junction (left) and schematic showing the introduction of a nanogap by the bending of a substrate (right) [93]. Reproduced with permission from [93]. Copyright 2006 Wiley-VCH Verlag GmbH & Co.

void, hillock, and whisker failures [96]. More recently the phenomenon has been exploited to create nanometer-sized gaps in conducting wires [87]. Electromigration results from the transfer of momentum from an electrical current to the atoms and ions of the conductor. The momentum causes the metal atoms to move and, at high enough current densities, the continuity of the wire is broken as gaps appear. The interest of electromigration to molecular electronics stems from the size of the gaps which can be on the order of a few nanometers. The importance of Joule heating in the migration of metal atoms should not be ignored [97, 98] as the temperature of gold wires exposed to the current densities necessary for gap creation can reach temperatures in excess of the melting point of the metal [99].

Electromigration-induced gaps can be inserted into gold wires deposited on an insulating substrate by ramping the current through the wire until the resistance suddenly increases [87]. Feedback loops coupled with a nonlinear current ramp provide additional control over the electrical current and resistive heating [100, 101] which yields a smaller spread in the gap sizes and more control over the device dimensions [100, 102–104]. Scanning and transmission electron microscopies have revealed the electromigration process *in situ* with real-time video [105, 106].

A significant concern with metal–molecule–metal junctions formed with electromigration gaps is the presence of residual metal clusters or metal islands remaining between the electrodes after the gap formation is complete. Electronic artifacts arising from the metal clusters can mask or mimic the electrical properties of the molecular component. Park's early studies with metal–molecule–metal junctions formed by electromigration techniques demonstrated Coulomb blockade and Kondo effects in chromium and vanadium complexes bridging the electrodes that are consistent with single-atom and single-molecule devices [6, 107]. However, subsequent experiments on pristine nanogaps formed by electromigration revealed that the apparent vacant junctions also exhibit Coulomb blockade and Kondo effects despite the absence of the molecular element [104, 108, 109]. Electrical artifacts stemming from the molecule-free nanogaps are attributed to the presence of magnetic impurities in the gold islands and gold clusters between the electrodes. The perceptible similarity in the electrical properties of the molecular components and metal clusters complicate the assignment of the Kondo effect's origin.

The early work with conventional electromigration gaps produced relatively low yields of nanogaps (∼10–20%) that provide measurable currents [6, 107, 110–112]. Moreover, each junction must be individually addressed during the fabrication process. Modifications of the electromigration procedure have yielded simpler and more reliable routes to fabricating arrays of nanogaps. Strachan and Johnson developed a strategy for fabricating vacant nanogaps in parallel using a feedback-controlled electromigration method [103]. The concurrent fabrication technique enables the generation of large arrays of nanospaced junctions. Similar fabrication methods were demonstrated to produce clean and particle-free junctions [113]. Interestingly, the formation of electromigration gaps continues after the bias is removed and the gold atoms relax with significant movement in the gold wire continuing [114]. Wires broken after the applied voltage is stopped tend to result in cleaner gaps lacking the metal clusters typical of the electromigration process. The electrode separations can be controlled with field-emission currents that move gold atoms to further reduce the gap size after it has already been introduced [115]. With a combination of nonlinear current ramps, feedback loops, and field-emission currents, arrays of electromigration gaps can be fabricated that exhibit near-identical electrical properties.

Perhaps, the most significant application of electromigration nanogaps is the construction of three-electrode molecular devices [6, 107, 110–112]. Introducing vacant gaps in gold wires deposited on a planar substrate allows the underlying material to serve as a third contact to the molecular component. Single-molecule transistors have been fabricated from electromigration junctions with a variety of organic and inorganic compounds serving as the channel material including redox active transition metal complexes and oligo(phenylene

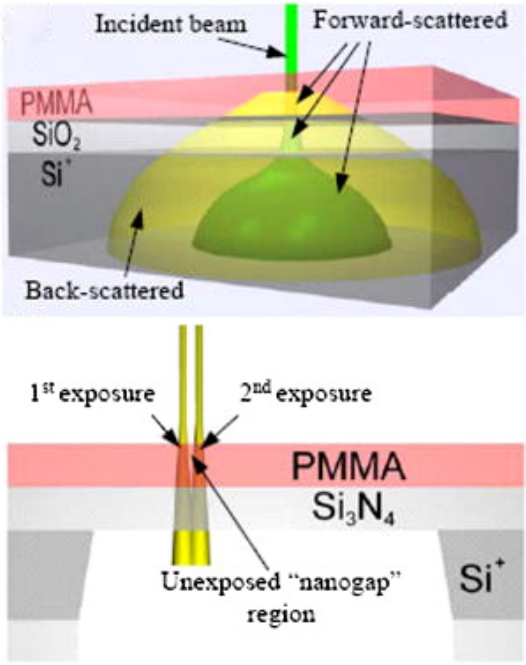

Figure 10. Back scattering from standard substrates (top) results in exposure of large sections of the PMMA resist. Thin Si_3N_4 substrates limit the exposure of the PMMA resist [12]. Reprinted with permission from [12]. Copyright 2006 American Institute of Physics.

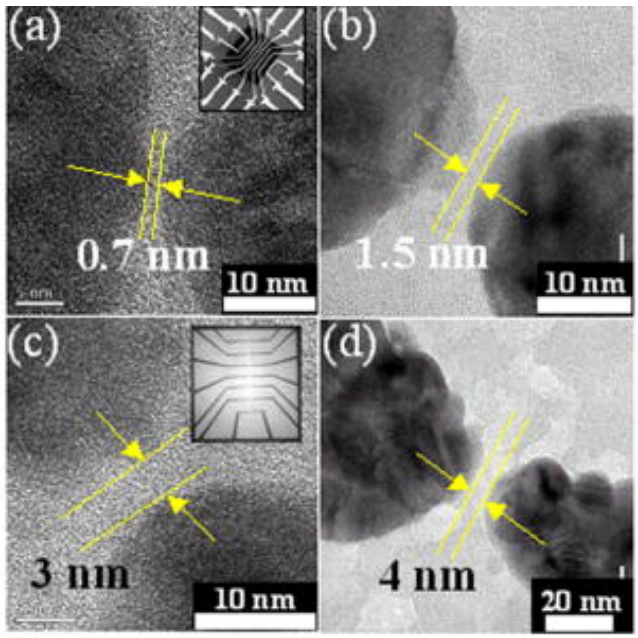

Figure 11. TEM of nanojunctions fabricated by electron-beam lithography with ultra-thin Si_3N_4 membranes. Inset in (a) and (c) show the full device with leads to external connections [12]. Reprinted with permission from [12]. Copyright 2006 American Institute of Physics.

ethynylene)s [6, 107, 110–112]. The redox properties of the transition metals and conjugated organics provide a rational mechanism for tuning the electronic structure and, hence, the conductance of the bridging molecule. In these experiments, gold wires are chemically modified with the molecular element prior to introducing the gaps via electromigration. After the current is ramped and the gap forms, a relatively small yield of devices (10–20%) exhibit electrical properties that are consistent with a metal–molecule–metal junction. The underlying gate electrode is used to toggle the conductance of the molecular bridge between on/off states. For example, the resistivity of polypyridyl cobalt complexes change by several orders of magnitude upon applying a gate voltage of 0.6 V [107]. However, the exact mechanism responsible for the observed switching is inconclusive [111], as the presence of gold clusters or particles in the electromigration gap has not been eliminated *vida supra* [104, 108, 109]. Additionally, the effect of the high temperature in the gold wire during the ramping of the electromigration current is likely to adversely affect the molecules adsorbed to the surface [97–99]. Any solid carbides that might form from deleterious chemical reactions between the molecular components and the gold electrodes or underlying substrate can also contribute electrical artifacts to the current profiles of the junctions.

3.3. Lithography

Integrated circuits containing hundreds of thousands or millions of nanogaps require a reliable and low-cost method for generating the metal electrodes with the necessary separations. Deep UV-photolithography offers an inexpensive approach for patterning metal electrodes but the available resolution limits feature sizes down to 50 nm. Conventional electron-beam lithography can push the limit to 10 nm. While these dimensions are still too large for measuring tunneling currents through single molecules, they are well suited for investigating the electronic properties of polymers, nanocrystals, and liquids [116–119]. Photolithographically patterned leads often serve as starting points for generating smaller molecular-sized gaps by depositing additional metal on the electrodes. Nanometer-sized features are possible with advanced lithographic techniques which adapt conventional photo- and electron-beam lithography for generating nanogaps with molecular dimensions.

Fischbein and Drndić developed a strategy for generating subnanometer features using conventional electron-beam lithography coupled with a thin-film substrate [12]. The resolution of electron-beam lithography is primarily limited by electron back scattering from the substrate [120, 121], figure 10. By utilizing a 100 nm thick silicon nitride membrane as the substrate, the back scattering of the electron-beam was considerably reduced allowing a significant improvement in the resolution of the irradiated area. Metal leads with subnanometer spacings can be patterned and imaged directly with a TEM using the thin membranes, figure 11. However, the thin substrates required for the transparent electron-beam lithography are very fragile and the prospects of scaling the technology for mass production necessitate a significant engineering effort.

Oblique angle shadow evaporation of metal vapor offers an alternative approach to constructing large arrays of

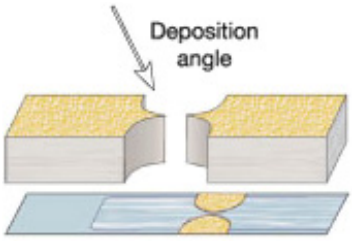

Figure 12. Oblique angle deposition with an elevated mask results in feature sizes that are smaller than those of the mask [89]. Reproduced with permission from [89]. Copyright 2003 Nature Publishing Group.

nanogaps for molecular electronics using less expensive photolithographic methods. In this approach [89, 122], the patterned features of a conventional photoresist are substantially improved by suspending the mask above the substrate and increasing the angle of the metal deposition from the surface normal, figure 12. An uneven substrate provides a similar effect as an elevated mask and can simplify the fabrication process [123, 124]. Two- [124] and three-terminal [89, 122, 123] molecular devices have been produced with a relatively simple strategy of tilting the substrate with a raised mask relative to the direction of the incoming metal vapor. With these techniques, gap distances of a few nanometers are possible and the final electrode separation is determined by the granularity of the metal deposits [124]. Substrates held at lower temperatures yield gap sizes that are closer to the expected dimensions due to the smaller grain size of the metal electrodes. Larger grains formed with higher substrate temperatures result in irregular surface features which can significantly change the electrode geometry.

Masks comprised of carbon nanotubes provide a highly controlled and scalable method for generating arrays of nanogaps. The millimeter length and uniform diameter of the nanotubes are conducive to fabricating large quantities of nanojunctions with identical geometries. Carbon nanotubes with diameters of 1–2 nm for single-walled nanotubes to 5–100 nm for multi-walled nanotubes can be used to directly pattern nanometer features on a substrate surface. Photoresists are used as supports to hold the nanotubes in place [125]. Arrays of nanogaps with separations of 0.8–2.3 nm are possible using the smaller single-walled nanotubes [126, 127] with device yields in excess of 80%. However, this technique does not provide any control over the exact placement of the nanotubes across the resist supports. Chen and coworkers [128] demonstrated the controlled placement of carbon nanotubes for constructing shadow masks designed to pattern large arrays of nanojunctions. A 2 MHz, 20 V AC electric field was used to direct the placement of carbon nanotubes dispersed in dilute solutions across micron-sized gaps separating metal electrodes. The metal electrode and carbon nanotube features serve as the mask for patterning nanometer-sized junctions, figure 13. Features patterned with carbon nanotube shadow masks are highly dependent on the incident angle of the metal vapor and gap sizes are often smaller than predicted by a direct line-of-sight deposition [129]. Presumably, surface migration of metal atoms is conditional on the incident angle of the vapor. The possibility of large-scale fabrication of nanogap arrays with the nanotube uniformity promises a straightforward route to vacant nanojunctions with dimensions that are ideally suited for molecular electronics.

3.4. Focused ion beam

Focused ion beams (FIB) can be used to etch away metal creating a gap in a wire or to deposit material narrowing the span of larger gaps (>10 nm) to a few nanometers. A well focused ion beam of Ga^+ can be condensed down to ∼10 nm, too large to directly pattern metal electrodes within tunneling distances. Shigeto *et al* employed Ga^+-beams to deposit tungsten from $W(CO)_6$ gas on the edges of a slit in a silicon nitride membrane [130]. As the Ga^+-beam rasters across the slit, tungsten deposits on the edges reducing the width of the slit. The resistance of the gap drops from an initial value in excess of 10 GΩ to 100–300 Ω during the fabrication process at which point the deposition is terminated. Separations between tungsten electrodes of <3 nm are possible with this approach, much less than the 10 nm Ga^+-beam diameter.

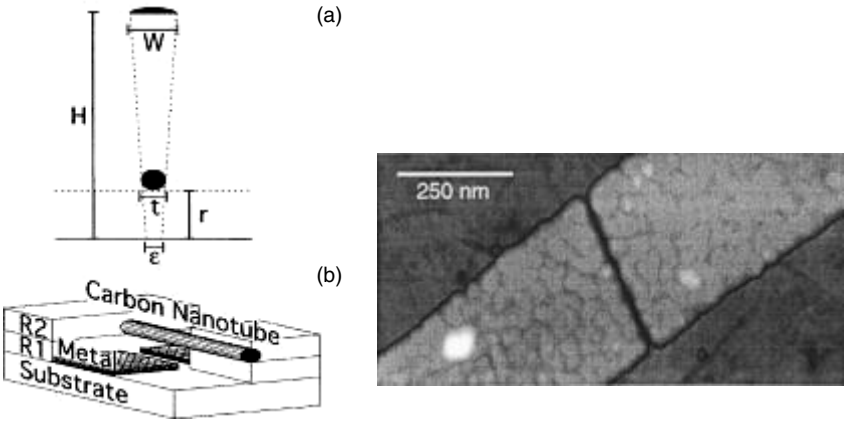

Figure 13. Shadow mask of a carbon nanotube suspended from the substrate using two layers of electron-beam resist (R1 and R2) (left). AFM micrograph of a nanogap formed with a carbon nanotube shadow mask [125]. Reproduced with permission from [125]. Copyright 2000 American Institute of Physics.

Focused Ga^+-beams have also been used to etch nanogaps into gold layers sandwiched between thin titanium films [131]. The titanium has a slower sputtering rate and prevents the tails in the ion beam from etching the gold. Combined with a feedback loop, gaps of 3 nm are possible with this technique and a Ga^+-beam diameter of 12 nm. The Ga^+-beams can leave gallium impurities in the junction as detected by Auger depth profiling. Iodine-assisted Ga^+ ion beam etches limit the Ga contamination to only 5% compared to 25% without I_2 [131]. Impurity concentrations must be limited in molecular-sized devices as contamination of a gap by a single-atom can compromise the electronic properties of the junction. This simple and straightforward approach to generating nanospaced electrodes has a 90% yield and is readily suitable for producing large arrays of nanojunctions.

3.5. Chemical and electrochemical deposition/dissolution

Chemical and electrochemical means of closing the distance between two lithographically patterned metal electrodes provides a relatively easy method for depositing metal atoms at well controlled rates. In these strategies, metal atoms from solution are deposited on prefabricated leads with micron or submicron separations by a chemical or electrochemical process. As metal deposits, the separation between the electrodes decreases. Limiting the metal deposition to only the desired sites is somewhat challenging using these procedures as the metal solution is in contact with the entire circuit. Ideally, the metal atoms only deposit on the surface of the leads by one atomic layer at a time to keep the metal electrodes at a uniform distance. However, surface defects and grain boundaries in the electrode causes an uneven accumulation of metal on the surface. Slow deposition rates can be maintained with dilute solutions or limiting the Faradaic current densities which aid in producing a more uniform coverage.

The deposition area is more difficult to control with electroless plating methods as the plating solution contains both the metal atoms and reducing agent needed to precipitate the solid metal. One strategy for controlling the deposition process is to localize a catalyst on the metal leads that are to be extended [132]. Gold leads separated by 1–2 μm were modified with 2-mercaptoethylamine which provides amino groups disposed away from the surface. The pendent amines bind a Pd(II) catalyst to the gold surface which catalyzes the deposition of metallic copper on the gold surfaces resulting in a decrease of the gap from a few micrometers to 45 nm [132]. Even smaller nanogaps (5 nm) were fabricated using medical solutions of iodine tincture, ascorbic acid, and $[AuI_4]^-$ [133]. The ascorbic acid reduces the gold in solution and is catalytically re-reduced at the gold electrodes. Thus, the gold leads catalyze the deposition of gold atoms from solution and accumulate metal on the surface.

Arrays of integrated nanogaps have been generated by the electroless plating of gold on patterned leads with separations of 18–52 nm from $HAuCl_4$ (aq) solutions and mild reducing agents (hydroxyl amine) [134]. By controlling the concentration of the hydroxyl amine and the reaction time, the final separation of the metal electrodes could be controlled within a few nanometers and with a narrower distribution of gap sizes, figure 14. As the leads come closer together, the catalytic properties of the metal surface in the vicinity of the gap are less accessible to the reactants in solutions. Consequently, the plating process slows as the electrodes approach tunneling distances. Device yields of 90% are reported; however, the spread in the final electrode separation is still fairly large at 3.3 ± 1.4 nm.

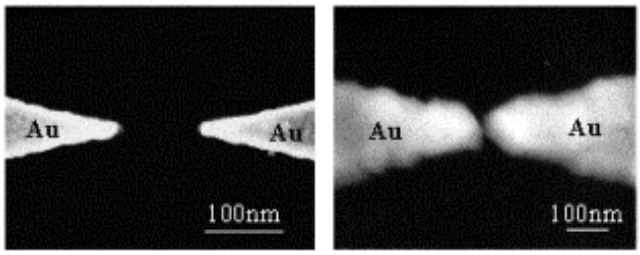

Figure 14. SEM images of gold electrodes before (left) and after (right) electroplating. The final gap size is 8 nm [136]. Reproduced with permission from [136]. Copyright 2003 Elsevier.

Electrochemical deposition/dissolution techniques offer a more precise method for directing the metal atoms to a specific lead. In this process, a potential applied on the lead induces metal atoms in solution to plate on the electrode. Only electrodes with the applied voltage deposit the additional material leaving the other electrodes in the array untouched. Additionally, if the gap becomes too small, the potential can be reversed to dissolve some of the electrode metal, thereby enlarging the gap [135, 136]. Quantized changes in tunneling currents occur as metal atoms deposit on the surface. However, the stepwise increase in current is much smaller than expected for a reduction in the gap size by one atomic layer [135]. Instead, the metal electrodes undergo a structural relaxation that changes the overall dimensions of the lead as new metal atoms are deposited [137].

As in the case with the deposition process for fabricating nanogaps such as FIB and shadow evaporation, the use of a feedback loop provides greater control over the dimensions of the tunneling junctions formed by electrodeposition/dissolution techniques. An overlapping AC signal can monitor the junction's resistance or admittance as the potentiostatic deposition occurs [136]. With a simple low-frequency feedback loop, gaps with subnanometer size are possible [138]. The final gap size depends on the frequency of the sinusoidal signal [7, 88, 139]. Changes in feedback signal collected at low frequencies (70 or 300 Hz) occur in quantum steps due to the increased tunneling between the electrodes [140]. By contrast, changes in the conductance monitored with a high-frequency feedback loops (3 kHz) increases continuously as the metal is plated. With the high-frequency monitoring, the deposition process can be stopped with large electrode separations that are on the order of tens of nanometers, well beyond conventional tunneling distances. At these distances, the feedback signal responds to changes in the junction's capacitive reactance. Metal can still be extended to further reduce the electrode separations to a molecule-sized dimensions or smaller [7]. As in the case of the

chemical deposition, there is little control over the specific morphology of the electrodes during the electrochemical plating sequence. Consequently, the cross-sectional area of the nanoelectrodes can undergo significant changes as material is deposited and removed. Moreover, changes in the electrode dimensions and surface area contribute to the overall conductance and capacitance of the gap. The feedback loop ensures the formation of nanogaps with precise electrical properties rather than a specific geometry (gap size and cross-sectional area).

3.6. Molecular and atomic rulers

Fabricating vacant nanogaps with a molecular or atomic ruler is similar to the top-contact approach for generating metal–molecule–metal junctions in that a molecular or atomic film of a specific size serves as a physical separator or template for constructing the nanospaced electrodes. Unlike the top-contact devices, the molecular or atomic ruler is not part of the final circuit. Instead, the ruler acts as a temporary spacer for constructing the metal electrodes and is removed after the electrodes are put into place leaving a vacant gap. With molecular rulers, the template dimensions are set by the length of the molecule or thickness of the atomic film used as the temporary spacer, such as a long alkyl chain or reactive oxide layer. The dimensions of the molecular ruler and resulting nanogap are controlled by simply changing the number of carbon atoms in the alkyl chain or the thickness of the oxide film. Molecular and atomic rulers that are sufficiently insulating may be only partially removed allowing space for the molecular element to assemble between the leads. The atomic rulers are typically deposited using electron-beam lithography which provides film thicknesses with Angstrom resolution. Since the metal electrodes are constructed around the template rulers, the dimensions of the atomic or molecular films are crucial to determining the width of the resulting nanogap. However, the final gap is unlikely to be exactly the size of the ruler element as the metal structures can relax after the molecular or atomic templates are removed.

The use of mercaptoalkanoic acids as molecular templates for fabricating nanogaps was first reported by Weiss [141]. The mercaptoalkanoic acids serve as a molecular resist for patterning gold features separated by the nanometer dimensions of the alkanoic acid, figure 15. Multiple acid layers can be added sequentially to increase the final electrode spacings [142, 143]. After Ti/Au deposition and liftoff of the mercaptoalkanoic acid resist, nanogap features are left with separations determined by the thickness of the mercaptoalkanoic acid layer [144]. Vacant nanogaps suitable for constructing metal–molecule–metal junctions are possible with a single layer of the molecular resist with device yields of 80% [145]. Arrays of molecular circuits comprising oligo(ethynyl phenylene)s have been generated using molecular ruler lithography [146]. Molecular ruler lithography is especially promising for molecular electronics applications since it provides a straightforward and inexpensive route to fabricating large arrays of nanospaced junctions with specific gap sizes that are highly reproducible.

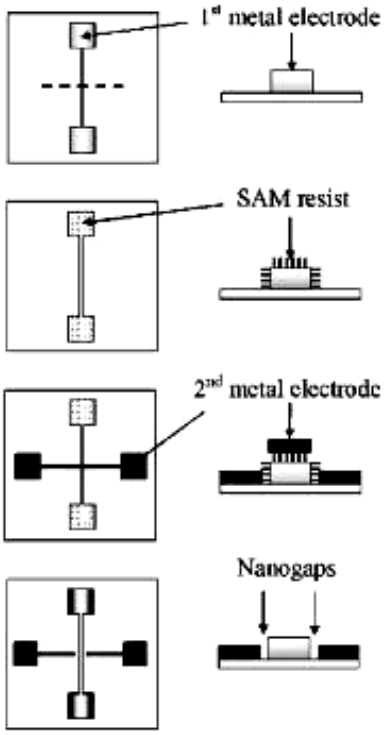

Figure 15. Fabrication process with molecular rulers: (top) initial electrode is deposited with electron-beam lithography, (second from top) molecular resist is adsorbed to patterned electrode, (second from bottom) second electrode is electron-beam deposited, and (bottom) molecular film is removed with stripper leaving nanogaps between the metal electrodes [145]. Reproduced with permission from [145]. Copyright 2006 American Institute of Physics.

Nanofabrication techniques based on atomic rulers are among the more recently developed strategies for generating nanospaced electrodes. Instead of using an organic molecule of a specific size as the templating agent, an inorganic film deposited with precise atomic thicknesses serves as a separator for the two metal leads. The inorganic film is removed after the metal electrodes are complete by a selective chemical etch. In some configurations, an insulating ruler film can be left in place or only partially removed to create an exposed cavity that provides architectural support for separating the metal leads. If the atomic film is only partially removed to reveal a nanogap, the support layer must be sufficiently insulating so as not to provide an alternative pathway for charge transfer. Point defects in a nanometer thick films can provide density of states comparable to molecular elements bridging the gap. Fortunately, the electrical properties of the nanogaps can be fully characterized prior to inserting the molecular element of interest. The structural integrity of the nanogaps should also be considered when studying charge transfer through nanoarchitectures that may deform with time or high current densities. Subtle changes in geometry or electrode separation can greatly affect tunneling currents.

For an atomic film to function as a temporary spacing layer separating metal electrodes, the templating material must be selectively removed leaving the metal electrode structures in nominally the same geometry. Gold and platinum electrodes

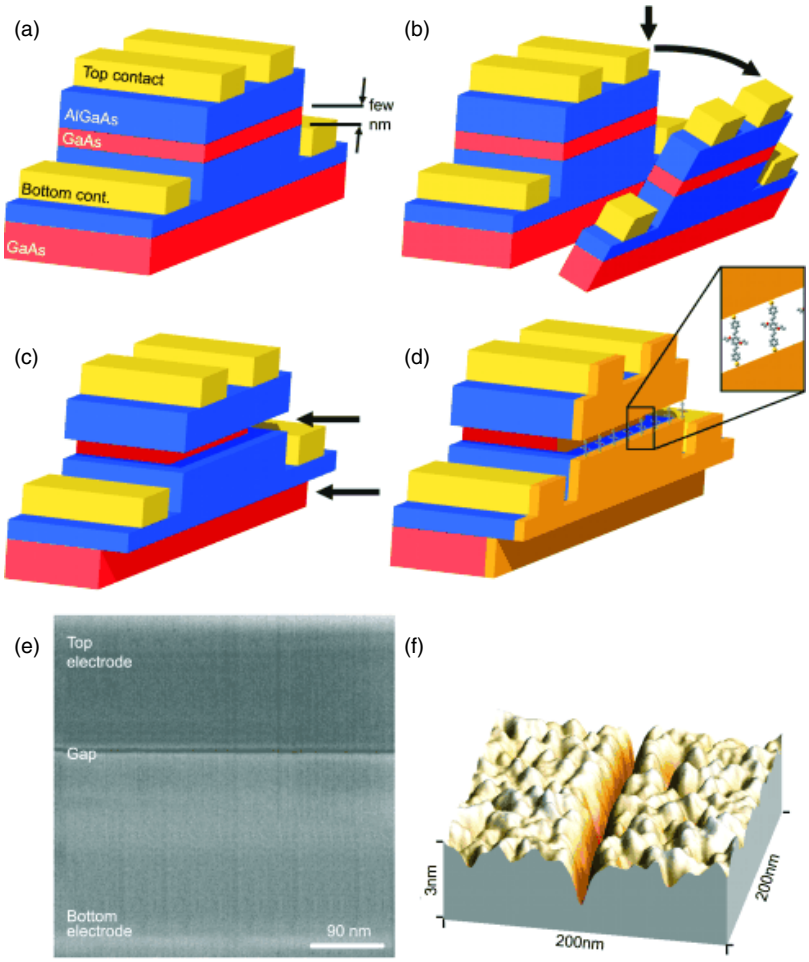

Figure 16. Fabrication scheme for generating vacant nanogaps with a AlGaAs/GaAs/AlGaAs trilayer: (a) AlGaAs/GaAs heterostructure is epitaxially grown with lithographically defined metal leads, (b) cleavage along crystal plane, (c) GaAs layer is selectively etched, and (d) metal film is deposited and molecular elements self-assemble in the gap. (e) SEM and (f) AFM of a heterostructure nanogap [151]. Reproduced with permission from [151]. Copyright 2007 Wiley-VCH Verlag GmbH & Co.

are robust enough to withstand harsh chemical etches and electrochemical stripping potentials that dissolve other metals serving as the atomic ruler. To adapt these techniques to constructing nanospaced electrodes from more reactive metals requires a compatible atomic layer and a chemical etch sequence that is relatively nonreactive with the metal leads. A variety of materials, conductors and insulators, have been demonstrated as suitable templates with standard methods for selective removal by chemical or electrochemical means [147–149].

The planar edge of metal–insulator–metal junctions can be used to connect molecular elements larger than the thickness of the insulating layer [150]. In these devices the traditional gap between the electrodes is replaced by two coplanar metal leads separated by a few nanometers. The appeal of this approach to constructing metal–molecule–metal devices is that the thickness of the insulating layer can be controlled with great precision down to subnanometer resolution. Electrical defects within the insulating layer can provide an alternative route for electron transfer and large cross-sectional areas at the metal–insulator–metal interface will compete with the molecular element as a tunneling pathway. Similar edge-on nanogaps have been fabricated with AlGaAs-GaAs-AlGaAs trilayers, figure 16 [151, 152]. The edge of the exposed GaAs layer is partially recessed-etched to create nanogaps between the AlGaAs electrodes while still providing structural support. Gold is subsequently deposited perpendicular to the planar layers resulting in metal electrodes on the AlGaAs phases that are separated by the thickness of the GaAs layer. Molecular elements self-assemble across the recessed GaAs gap and complete the nanocircuit [150, 151].

Integrated arrays of nanogaps can be generated using conventional nanofabrication techniques in conjunction with the selective removal of an atomic support layers. For example, islands of Si/SiO_2 on a silicon substrate serve as the basis for constructing nanospaced gold electrodes, figure 17 [153]. After the silicon oxide is selectively removed, the gold electrodes remain with separations that are on the order of a few nanometers depending on the original thickness of the oxide and gold layers. Integrated cross point structures with Pt wires and 3 nm thick Al/AlO_x supports have been reported by Chen, figure 18 [154]. The Al/AlO_x layer is partially removed with a phosphoric acid solution leaving an undercut support which can be bridged by oligo(phenylene ethynylene)

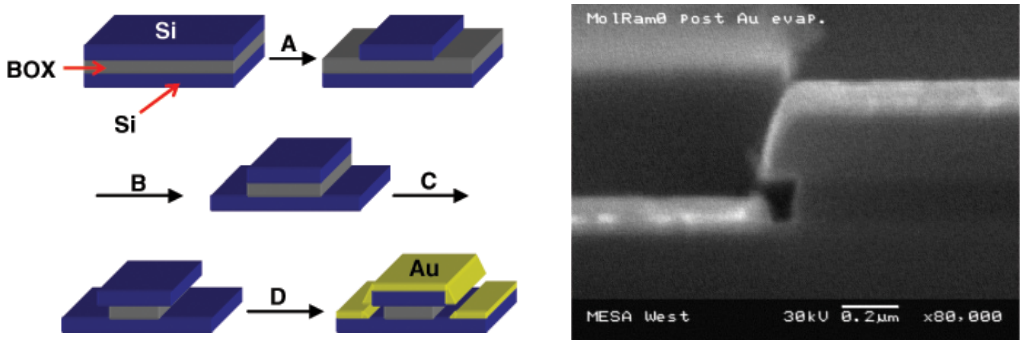

Figure 17. Fabrication process (left) of vacant nanogap junctions by recessed chemical etch of a buried silicon oxide layer (BOX): (A) top silicon layer is etched, (B) buried oxide layer is etched, (C) wet etching of oxide layer to create an undercut, and (D) deposition of gold film. SEM image (right) of nanogap formed after gold deposition [153]. Reproduced with permission of [153]. Copyright 2005, IOP Publishing Limited.

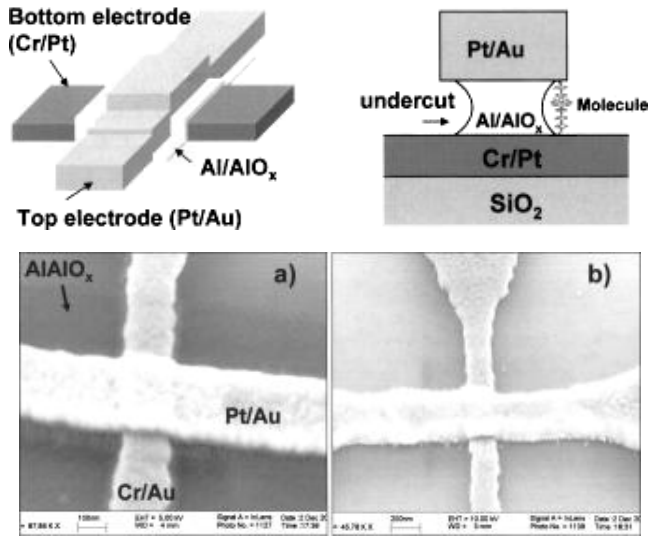

Figure 18. Recessed etch of Al/AlO$_x$ layer in a cross point structure (top) leaves vacant nanogaps for molecular bridges. SEM micrographs before (a) and after (b) chemical etching [154]. Reprinted with permission from [154]. Copyright 2006 AVS Science & Technology.

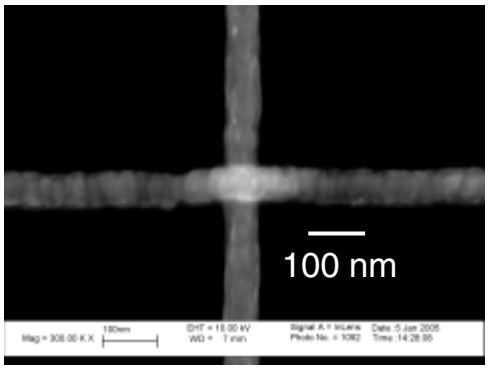

Figure 19. SEM image of a vacant crossbar node of gold fabricated by selective chemical etching of the intervening chromium layer [155]. Reproduced with permission from [155]. Copyright 2007, American Chemical Society.

structures. Interestingly, the leakage resistance of a Al/AlO$_x$ junction comprised of two 200 nm wide wires reduces from 10^{12} Ω to 10^{11} Ω upon removal of the oxide. Metal–molecule–metal junctions formed with these undercut supports and the oligo(phenylene ethynylene)s exhibit resistances on the order of 10^8–10^{10} Ω. Device yields with the Al/AlO$_x$ rulers are in excess of 70%. Importantly, the undercut SiO$_2$ and Al/AlO$_x$ supported junctions are easily configured into extended arrays of nanojunctions using readily available instrumentation.

Vacant nanocrossbar arrays were fabricated in our laboratory using a selective chemical etch to remove an intervening chromium layer between orthogonal gold wires, figure 19 [155]. Complete removal of the conducting chromium support increases the junction resistance by approximately eight orders of magnitude. A silicon oxide mesh is sputtered around the crossbar intersections to anchor the top gold wires to the array. The thickness of the chromium layers is on the order of a few nanometers. However, fits to the tunneling curves acquired with the vacant nanojunctions generally requires somewhat smaller gaps than expected for a gap based on the original thickness of the Cr layer. Presumably, the vacant gold structures relax with a slight adjustment in their geometry and separation. With a 12 × 12 array of nanogaps constructed from a nominally uniform chromium film separating 200 nm wide gold wires, the tunneling currents span only one order of magnitude, figure 20. Current variations of this order correlate to metal–metal distance variations of 0.4 nm, slightly larger than the diameter of a single gold atom. Slight differences in wire widths likely contribute to some of the current variation. The narrow size distribution of the vacant crossbar nanogaps demonstrates that large arrays of integrated molecular-sized junctions are possible with the necessary geometry and consistency required for molecular electronics.

4. Conclusions

Over the last decade several approaches for fabricating nanospaced electrodes have been successfully developed for studying electron tunneling through molecular ensembles.

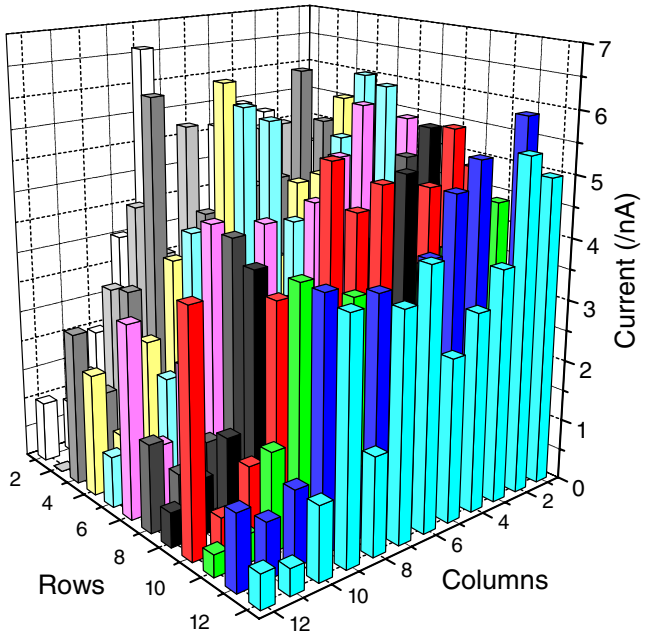

Figure 20. Steady-state currents for a 12 × 12 crossbar array constructed with gold wires initially separated by 3 nm of chromium. The voltage at each node is held at 0.5 V.

Most significantly, arrays of junctions with consistent and reproducible electronic properties are now possible. Molecular switches have been configured into working circuits and demonstrated memory and logic functions. Yet, considerable work on nanoelectrode fabrication is still needed before the full benefits of molecular electronics can be realized. For example, relatively few studies have focused on reducing the cross-sectional areas of molecular junctions which are often several orders-of-magnitude larger than the molecular elements themselves. Without improvements in the size of the metal leads, the dimensions of the molecular circuits expand beyond that currently available with silicon technology and deep UV-photolithography. As the electrodes become smaller, the morphology of the metal can play a significant role in determining the reliability of a fabrication process as individual grains in the metal leads dominate the device structure and performance. Further advances in nanospaced electrodes fabrication will likely address these issues and yield electronic circuits that are an order-of-magnitude smaller than current technology.

To date, the most accomplished molecular circuitry relies on top contacts that are thermally deposited on SAM or LB films [45, 46]. The mechanism responsible for conductivity switching in these devices remains ambiguous and the effects of filament formation and metal ion migration within the nanogaps are poorly understood. In order to take full advantage of a molecule's intrinsic properties, electronic artifacts arising from the metal leads must be identified and conditions found in which the metal electrodes do not contribute significantly to the gap's electrical response. Until these nonmolecular effects are controlled, the switching properties of a molecular circuit are likely to be convoluted with the electrical response of the leads and dependent on the method of their fabrication.

Acknowledgments

This work was funded by the Office of Naval Research. The research described in this paper was carried out partly at the Jet Propulsion Laboratory, California Institute of Technology, under contract with the National Aeronautics and Space Administration.

References

[1] Likharev K K 2003 *Nano and Giga Challenges in Microelectronics* ed J Greer, A Korkin and J Labanowski (Amsterdam: Elsevier)
[2] Aviram A and Ratner M A 1974 Molecular rectifiers *Chem. Phys. Lett.* **29** 277–83
[3] Tao N J 2006 Electron transport in molecular junctions *Nat. Nanotechnol.* **1** 173–81
[4] Lu W and Lieber C M 2007 Nanoelectronics from the bottom up *Nat. Mater.* **6** 841–50
[5] Reed M A, Zhou C, Muller C J, Burgin T P and Tour J M 1996 Conductance of a molecular junction *Science* **278** 252–4
[6] Liang W, Shores M P, Bockrath M, Long J R and Park H 2002 Kondo resonance in a single-molecule transistor *Nature* **417** 725–8
[7] Qing Q, Chen F, Li P G, Tang W H, Wu Z Y and Liu Z F 2005 Finely tuning metallic nanogap size with electrodeposition by utilizing high-frequency impedance in feedback *Angew. Chem. Int. Edn* **44** 7771–5
[8] Fischbein M D and Drndic M 2007 Sub-10 nm device fabrication in a transmission electron microscope *Nano Lett.* **7** 1329–37
[9] Venkataraman L, Klare J E, Nuckolls C, Hybertsen M S and Steigerwald M L 2006 Dependence of single-molecule junction conductance on molecular conformation *Nature* **442** 904–7
[10] Kushmerick J G, Naciri J, Yang J C and Shashidhar R 2003 Conductance scaling of molecular wires *Nano Lett.* **3** 897–900
[11] Haag R, Rampi M A, Holmlin R E and White H S 1999 Electrical breakdown of aliphatic and aromatic self-assembled monolayers used as nanometer-thick organic dielectrics *J. Am. Chem. Soc.* **121** 7895–906
[12] Fischbein M D and Drndic M 2006 Nanogaps by direct lithography for high-resolution imaging and electronic characterization of nanostructures *Appl. Phys. Lett.* **88** 063116
[13] Gergel-Hakett N *et al* 2006 Effects of molecular environments on the electrical switching with memory of nitro-containing OPEs *J. Vac. Sci. Technol.* A **24** 1243–8
[14] Long D P, Patterson C H, Moore M H, Seferos D S, Bazan G C and Kushmerick J G 2005 Magnetic directed assembly of molecular junctions *Appl. Phys. Lett.* **86** 153105
[15] Ramachandran G K *et al* 2003 Electron transport properties of a carotene molecule in a metal–(single molecule)–metal junction *J. Phys. Chem.* B **107** 6162–9
[16] Galperin M, Ratner M A and Nitzan A 2007 Molecular transport junctions: vibrational effects *J. Phys.: Condens. Matter* **19** 103201
[17] Datta S, Tian W, Hong S, Reifenberger R, Henderson J I and Kubiak C P 1997 Current–voltage characteristics of self-assembled monolayers by scanning tunneling microscoy *Phys. Rev. Lett.* **79** 2530–3
[18] Tian W, Datta S, Hong S, Reifenberger R, Henderson J I and Kubiak C P 1998 Conductance spectra of molecular wires *J. Chem. Phys.* **109** 2874–82

[19] Wiesendanger R and Güntherodt H-J (ed) 1996 *Scanning Tunneling Microscopy III: Theory of STM and Related Scanning Probe Methods* (New York: Springer)
[20] Bonnell D A (ed) 1993 *Scanning Tunneling Microscopy and Spectroscopy: Theory, Techniques, and Applications* (New York: VCH)
[21] Dhirani A, Lin P-H, Guyot-Sionnest P, Zehner R W and Sita L R 1997 Self-assembled molecular rectifiers *J. Chem. Phys.* **106** 5249–53
[22] Lewis P A, Inman C E, Yao Y, Tour J M, Hutchison J E and Weiss P S 2004 Mediating stochastic switching of single molecules using chemical functionality *J. Am. Chem. Soc.* **126** 12214–5
[23] Bumm L A, Arnold J J, Dunbar T D, Allara D L and Weiss P S 1999 Electron transfer through organic molecules *J. Phys. Chem.* B **103** 8122–7
[24] Dürig U, Züger O, Michel B, Häussling L and Ringsdorf H 1993 Electronic and mechanical characterization of self-assembled alkanethiol monolayers by scanning tunneling microscopy combined with interaction-force-gradient sensing *Phys. Rev.* B **48** 1711–7
[25] Chen I-W, Fu M-D, Tseng W H, Chen C-h, Chou C-M and Luh T-Y 2007 The effect of molecular conformation on single molecule conductance: measurements of π-conjugated oligoaryls by STM break junction *Chem. Commun.* 3074–6
[26] Fan F R F, Yang J P, Cai L T, Price D W, Dirk S M, Kosynkin D V, Yao Y X, Rawlett A M, Tour J M and Bard A J 2002 Charge transport through self-assembled monolayers of compounds of interest in molecular electronics *J. Am. Chem. Soc.* **124** 5550–60
[27] Beebe J M, Engelkes V B, Liu J Q, Gooding J, Eggers P K, Jun Y, Zhu X Y, Paddon-Row M N and Frisbie C D 2005 Length dependence of charge transport in nanoscopic molecular junctions incorporating a series of rigid thiol-terminated norbornylogs *J. Phys. Chem.* B **109** 5207–15
[28] Wakamatsu S, Fujii S, Akiba U and Fujihara M 2006 Length dependence of tunneling current through single phenylene oligomers measured by scanning tunneling microscopy at low temperature *Japan. J. Appl. Phys.* 1 **45** 2736–42
[29] Wassel R A, Credo G M, Fuierer R R, Feldheim D L and Gorman C B 2004 Attenuating negative differential resistance in an electroactive self-assembled monolayer-based junction *J. Am. Chem. Soc.* **126** 295–300
[30] Wang S C, Lu W C, Zhao Q Z and Bernholc J 2006 Resonant coupling and negative differential resistance in metal/ferrocenyl alkanethiolate/STM structures *Phys. Rev.* B **74** 195430
[31] Pi U H, Jeong M S, Kim J H, Yu H Y, Park C W, Lee H and Choi S-Y 2005 Current flow through different phases of dodecanethiol self-assembled monolayer *Surf. Sci.* **583** 88–92
[32] Moore A M, Mantooth B A, Donhauser Z J, Yao Y, Tour J M and Weiss P S 2007 Real-time measurements of conductance switching and motion of single oligo(phenylene ethynylene) molecules *J. Am. Chem. Soc.* **129** 10352–3
[33] Moore A M, Dameron A A, Mantooth B A, Smith R K, Fuchs D J, Ciszek J W, Maya F, Yao Y, Tour J M and Weiss P S 2006 Molecular engineering and measurements to test hypothesized mechanisms in single molecule conductance switching *J. Am. Chem. Soc.* **128** 1959–67
[34] He J, Fu Q, Lindsay S, Ciszek J W and Tour J M 2006 Electrochemical origin of voltage-controlled molecular conductance switching *J. Am. Chem. Soc.* **128** 14828–35
[35] Wu S W, Ogawa N and Ho W 2006 Atomic-scale coupling of photons to single-molecule junctions *Science* **312** 1362–5
[36] Jäckel F, Wang Z, Watson M D, Mullen K and Rabe J P 2004 Prototypical single-molecule transistors with supramolecular gates: varying dipole orientation *Synth. Met.* **146** 269–72
[37] Lewis P A, Inman C E, Maya F, Tour J M, Hutchison J E and Weiss P S 2005 Molecular engineering of the polarity and interactions of molecular electronic switches *J. Am. Chem. Soc.* **127** 17421–6
[38] Donhauser Z J *et al* 2001 Conductance switching in single molecules through conformational changes *Science* **292** 2303–7
[39] Engelkes V B, Beebe J M and Frisbie C D 2004 Length-dependent transport in molecular junctions based on SAMs of alkanethiols and alkanedithiols: effect of metal work function and applied bias on tunneling efficiency and contact resistance *J. Am. Chem. Soc.* **126** 14287–96
[40] Suzuki M, Fujii S and Fujihira M 2006 Measurements of currents through single molecules of alkanedithiols by repeated formation of break junction in scanning tunneling microscopy under ultrahigh vacuum *Japan. J. Appl. Phys.* 1 **45** 2041–4
[41] Li X L, Xu B Q, Xiao X Y, Hihath J and Tao N J 2005 Measurement of electron transport properties of single molecules *Japan. J. Appl. Phys.* 1 **44** 5344–7
[42] Fujihira M, Suzuki M, Fujii S and Nishikawa A 2006 Currents through single molecular junction of Au/hexanedithiolate/Au measured by repeated formation of break junction in STM under UHV: effects of conformational change in an alkylene chain from gauche to trans and binding sites of thiolates on gold *Phys. Chem. Chem. Phys.* **8** 3876–84
[43] Nishikawa A, Tobita J, Kato Y, Fujii S, Suzuki M and Fujihira M 2007 Accurate determination of multiple sets of single molecular conductance of Au/1,6-hexanedithiol/Au break junctions by ultra-high vacuum-scanning tunneling microscope and analyses of individual current-separation curves *Nanotechnology* **18** 1–10
[44] Seferos D S, Blum A S, Kushmerick J G and Bazan G C 2006 Single-molecule charge-transport measurements that reveal technique-dependent perturbations *J. Am. Chem. Soc.* **128** 11260–7
[45] Collier C P, Mattersteig G, Wong E W, Luo Y, Beverly K, Sampaio J, Raymo F M, Stoddart J F and Heath J R 2000 A [2]catenane-based solid state electronically reconfigurable switch *Science* **289** 1172–5
[46] Collier C P, Wong E W, Belohradsky M, Raymo F M, Stoddart J F, Kuekes P J, Williams R S and Heath J R 1999 Electronically configurable molecular-based logic gates *Science* **285** 391–4
[47] Chen Y, Jung G Y, Ohlberg D A A, Li X M, Stewart D R, Jeppesen J O, Nielsen K A, Stoddart J F and Williams R S 2003 Nanoscale molecular-switch crossbar circuits *Nanotechnology* **14** 462–8
[48] Konstadinidis K, Zhang P, Opila R L and Allara D L 1995 An *in situ* x-ray photoelectron study of the interaction between vapor-deposited Ti atoms and functional groups at the surfaces of self-assembled monolayers *Surf. Sci.* **338** 300
[49] Tighe T B, Daniel T A, Zhu Z, Uppili S, Winograd N and Allara D L 2005 Evolution of the interface and metal film morphology in the vapor deposition of Ti on Hexadecanethiolate hydrocarbon monolayers on Au *J. Phys. Chem.* B **109** 21006–14
[50] Chang S C, Li Z Y, Lau C N, Larade B and Williams R S 2003 Investigation of a model molecular-electronic rectifier with an evaporated Ti-metal top contact *Appl. Phys. Lett.* **83** 3198–200
[51] Walker A V, Tighe T B, Haynie B C, Uppili S, Winograd N and Allara D L 2005 Chemical pathways in the interactions of reactive metal atoms with organic surfaces: vapor deposition of Ca and Ti on a methoxy-terminated alkanethiolate monolayer on Au *J. Phys. Chem.* B **109** 11263–72

[52] Nagy G and Walker A V 2006 Dynamics of the interaction of vapor-deposited copper with alkanethiolate monolayers: bond insertion, complexation, and penetration pathways *J. Phys. Chem.* B **110** 12543–54
[53] Stewart D R, Ohlberg D A A, Beck P A, Chen Y, Williams R S, Jeppesen J O, Nielsen K A and Stoddart J F 2004 Molecule-independent electrical switching in Pt/organic monolayer/Ti devices *Nano Lett.* **4** 133–6
[54] Lau C N, Stewart D R, Bockrath M and Williams R S 2005 Scanned probe imaging of nanoscale conducting channels in Pt/alkanoic acid monolayer/Ti devices *Appl. Phys.* A **80** 1373–8
[55] Ssenyange S, Yan H and McCreery R L 2006 Redox-driven conductance switching via filament formation and dissolution in carbon/molecule/TiO_2/Ag molecular electronic junctions *Langmuir* **22** 10689–96
[56] Lau C N, Stewart D R, Williams R S and Bockrath M 2004 Direct observation of nanoscale switching centers in metal/molecule/metal structures *Nano Lett.* **4** 569–72
[57] Karthäuser S, Lüssem B, Weides M, Alba M, Besmehn A, Oligschlaeger R and Waser R 2006 Resistive switching of rose bengal devices: a molecular effect? *J. Appl. Phys.* **100** 094504
[58] Koo J R, Pyo S W, Kim J H, Jung S Y, Yoon S S, Kim T W, Choi Y H and Kim Y K 2006 Current–voltage (I–V) characteristics of the molecular electronic devices using various organic molecules *Synth. Met.* **156** 86–9
[59] Fan X, Rogow D L, Swanson C H, Tripathi A and Oliver S R J 2007 Contact printed Co/insulator/Co molecular junctions *Appl. Phys. Lett.* **90** 163114
[60] Zhu Z, Daniel T A, Maitani M, Cabarcos O M, Allara D L and Winograd N 2006 Controlling gold atom penetration through alkanethiolate self-assembled monolayers on Au{111} by adjusting terminal group intermolecular interactions *J. Am. Chem. Soc.* **128** 13710–9
[61] Blackstock J J, Stickle W F, Donley C L, Stewart D R and Williams R S 2007 Internal structure of a molecular junction device: chemical reduction of PtO_2 by Ti evaporation onto an interceding organic monolayer *J. Phys. Chem.* C **111** 16–20
[62] Donley C L, Blackstock J J, Stickle W F, Stewart D R and Williams R S 2007 *In situ* infrared spectroscopy of buried organic monolayers: Influence of the substrate on titanium reactivity with a Langmuir–Blodgett film *Langmuir* **23** 7620–5
[63] Chen J, Reed M A, Rawlett A M and Tour J M 1999 Large on–off ratios and negative differential resistance in a molecular electronic device *Science* **286** 1550–2
[64] Zhou C, Deshpande M R, Reed M A, Jones II L and Tour J M 1997 Nanoscale metal/self-assembled monolayer/metal heterostructures *Appl. Phys. Lett.* **71** 611–3
[65] Wang W, Lee T, Kretzschmar I and Reed M A 2004 Inelastic electron tunneling spectroscopy of an alkanedithiol self-assembled monolayer *Nano Lett.* **4** 643–6
[66] Kushmerick J G, Blum A S and Long D P 2006 Metrology for molecular electronics *Anal. Chim. Acta* **568** 20–7
[67] Wold D J and Frisbie C D 2001 Fabrication and characterization of metal–molecule–metal junctions by conducting probe atomic force microscopy *J. Am. Chem. Soc.* **123** 5549–56
[68] Salomon A, Cahen D, Lindsay S, Tomfohr J, Engelkes V B and Frisbie C D 2003 Comparison of electronic transport measurements on organic molecules *Adv. Mater.* **15** 1881–90
[69] Andres R P, Bein T, Dorogi M, Feng S, Henderson J I, Kubiak C P, Mahoney W, Osifchin R G and Reifenberger R 1996 'Coulomb staircase' at room temperature in a self-assembled molecular nanostructure *Science* **272** 1323–5
[70] Morita T and Lindsay S 2007 Determination of single molecule conductances of alkanedithiols by conducting-atomic force microscopy with large gold nanoparticles *J. Am. Chem. Soc.* **129** 7262–3
[71] Na J S, Ayres J, Chandra K L, Chu C, Gorman C B and Parsons G N 2007 Conduction mechanisms and stability of single molecule nanoparticle/molecule/nanoparticle junctions *Nanotechnology* **18** 035203
[72] Bezryadin A, Dekker C and Schmid G 1997 Electrostatic trapping of single conducting nanoparticles between nanoelectrodes *Appl. Phys. Lett.* **71** 1273–5
[73] So H-M, Park J-W, Won D-J, Yun W S, Kang Y, Lee C, Kim J-J and Kim J 2004 Single-electron tunneling behavior of organic-molecule-based electronic devices *Japan. J. Appl. Phys.* **43** 6503–6
[74] Hong S H, Kim H K, Cho K H, Hwang S W, Hwang J S and Ahn D 2006 Fabrication of single electron transistors with molecular tunnel barriers using ac dielectrophoresis technique *J. Vac. Sci. Technol.* B **24** 136–8
[75] Rampi M A, Schueller O J A and White H S 1998 Alkanethiol self-assembled monolayers as the dielectric of capacitors with nanoscale thickness *Appl. Phys. Lett.* **72** 1781–3
[76] York R L and Slowinski K 2003 Tunneling conductivity of one-and two-component alkanethiol bilayers in Hg–Hg junctions *J. Electroanal. Chem.* **550** 327–36
[77] Holmlin R E, Haag R, Chabinyc M L, Ismagilov R F, Cohen A E, Terfort A, Rampi M A and White H S 2001 Electron transport through thin organic films in metal–insulator–metal junctions based on self-assembled monolayers *J. Am. Chem. Soc.* **123** 5075–85
[78] Rampi M A and White H S 2002 A versatile experimental approach for understanding electron transport through organic materials *Chem. Phys.* **281** 373–91
[79] Chabinyc M L, Chen X X, Holmlin R E, Jacobs H, Skulason H, Frisbie C D, Mujica V, Ratner M A, Rampi M A and Whitesides G M 2002 Molecular rectification in a metal–insulator–metal junction based on self-assembled monolayers *J. Am. Chem. Soc.* **124** 11730–6
[80] Galperin M, Nitzan A, Sek S and Majda M 2003 Asymmetric electron transmission across asymmetric alkanethiol bilayer junctions *J. Electroanal. Chem.* **550** 337–50
[81] Weiss E A, Chiechi R C, Kaufman G K, Kriebel J K, Li Z, Duati M, Rampi M A and Whitesides G A 2007 Influence of defects on the electrical characteristics of mercury-drop junctions: self-assembled monolayers of n-alkanethiolates on rough and smooth silver *J. Am. Chem. Soc.* **129** 4336–49
[82] York R L, Nacionales D and Slowinski K 2005 Electrical resistivity of monolayers and bilayers of alkanethiols in tunnel junction with gate electrode *Chem. Phys.* **319** 235–42
[83] Tran E, Rampi M A and Whitesides G M 2004 Electron transfer in a Hg-SAM//SAM-Hg junction mediated by redox centers *Angew. Chem. Int. Edn* **43** 3835–9
[84] Tran E, Grave C, Whitesides G A and Rampi M A 2005 Controlling the electron transfer mechanism in metal–molecules–metal junctions *Electrochim. Acta* **50** 4850–6
[85] Liu Y J and Yu H Z 2003 Alkyl monolayer passivated metal-semiconductor diodes: 2: comparison with native silicon oxide *Chemphyschem* **4** 335–42
[86] Sze S M (ed) 1998 *Modern Semiconductor Device Physics* (New York: Wiley)
[87] Park H, Lim A K L, Alivisatos A P, Park J and McEuen P L 1999 Fabrication of metallic electrodes with nanometer separation by electromigration *Appl. Phys. Lett.* **75** 301–3
[88] Chen F, Qing Q, Ren L, Wu Z Y and Liu Z F 2005 Electrochemical approach for fabricating nanogap electrodes with well controllable separation *Appl. Phys. Lett.* **86** 123105

[89] Kubatkin S, Danilov A, Hjort M, Cornil J, Brédas J-L, Stuhr-Hansen N, Hedegård P and Bjørnholm T 2003 Single-electron transistor of a single organic molecule with access to several redox states *Nature* **425** 698–701
[90] Gazzadi G C, Angeli E, Facci P and Frabboni S 2006 Electrical characterization and Auger depth profiling of nanogap electrodes fabricated by I-2-assisted focused ion beam *Appl. Phys. Lett.* **89** 173112
[91] Mimura K, Ara M and Tada H 2007 Preparation of nanogap electrodes of silicon by chemical etching *Mol. Cryst. Liq. Cryst.* **472** 453–7
[92] Hsueh C-C, Lee M-T, Freund M S and Ferguson G S 2000 Electrochemically directed self-assembly of gold *Angew. Chem. Int. Edn* **39** 1227–30
[93] Lörtscher E, Ciszek J W, Tour J M and Riel H 2006 Reversible and controllable switching of a single molecule junction *Small* **2** 973–7
[94] Grüter L, Gonzalez M T, Huber R, Calame M and Schonenberger C 2005 Electrical conductance of atomic contacts in liquid environments *Small* **1** 1067–70
[95] Giacalone F *et al* 2007 Tetrathiafulvalene-based molecular nanowires *Chem. Commun.* 4854–6
[96] Ho P S and Kwok T 1989 *Rep. Prog. Phys.* **52** 301
[97] Trouwborst M L, van der Molen S J and van Wees B J 2006 The role of Joule heating in the formation of nanogaps by electromigration *J. Appl. Phys.* **99** 114316
[98] Esen G and Fuhrer M S 2005 Temperature control of electromigration to form gold nanogap junctions *Appl. Phys. Lett.* **87** 263101
[99] Ramachandran G K, Edelstein M D, Blackburn D L, Suehle J S, Vogel E M and Richter C A 2005 Nanometre gaps in gold wires are formed by thermal migration *Nanotechnology* **16** 1294–9
[100] Strachan D R, Smith D E, Johnston D E, Park T H, Therien M J, Bonnell D A and Johnson A T 2005 Controlled fabrication of nanogaps in ambient environment for molecular electronics *Appl. Phys. Lett.* **86** 043109
[101] Mahapatro A K, Ghosh S and Janes D B 2006 Nanometer scale electrode separation (nanogap) using electromigration at room temperature *IEEE Trans. Nanotechnol.* **5** 232–6
[102] Wu Z M, Steinacher M, Huber R, Calame M, van der Molen S J and Schonenberger C 2007 Feedback controlled electromigration in four-terminal nanojunctions *Appl. Phys. Lett.* **91** 053118
[103] Johnston D E, Strachan D R and Johnson A T C 2007 Parallel fabrication of nanogap electrodes *Nano Lett.* **7** 2774–7
[104] Houck A A, Labaziewicz J, Chan E K, Folk J A and Chuang I L 2005 Kondo effect in electromigrated gold break junctions *Nano Lett.* **5** 16685–8
[105] Taychatanapat T, Bolotin K I, Kuemmeth F and Ralph D C 2007 Imaging electromigration during the formation of break junctions *Nano Lett.* **7** 652–6
[106] Heersche H B, Lientschnig G and O'Neill K 2007 *In situ* imaging of electromigration-induced nanogap formation by transmission electron microscopy *Appl. Phys. Lett.* **91** 072107
[107] Park J *et al* 2002 Coulomb blockade and the Kondo effect in single-atom transistors *Nature* **417** 722–5
[108] Sordon R, Balasubramanian K, Burghard M and Kern K 2005 Coulomb blockade phenomena in electromigration break junctions *Appl. Phys. Lett.* **87** 013106
[109] Heersche H B, de Groot Z, Folk J A, Kouwenhoven L P, van der Zant H S J, Houck A A, Labaziewicz J and Chuang I L 2006 Kondo effect in the presence of magnetic impurities *Phys. Rev. Lett.* **96** 017205
[110] Noguchi Y, Nagase T, Ueda R, Kamikado T, Kubota T and Mashiko S 2007 Fowler–Nordheim tunneling in electromigrated break junctions with porphyrin molecules *Japan. J. Appl. Phys.* 1 **46** 2683–6
[111] Keane Z K, Ciszek J W, Tour J M and Natelson D 2006 Three-terminal devices to examine single-molecule conductance switching *Nano Lett.* **6** 1518–21
[112] Natelson D, Yu L H, Ciszek J W, Keane Z K and Tour J M 2006 Single-molecule transistors: electron transfer in the solid state *Chem. Phys.* **324** 267–75
[113] Strachan D R, Smith D E, Fischbein M D, Johnston D E, Guiton B S, Drndic M, Bonnell D A and Johnson A T 2006 Clean electromigrated nanogaps imaged by transmission electron microscopy *Nano Lett.* **6** 441–4
[114] O'Neill K, Osorio E A and van der Zant H S J 2007 Self-breaking in planar few-atom Au constrictions for nanometer-spaced electrodes *Appl. Phys. Lett.* **90** 133109
[115] Kayashima S, Takahashi K, Motoyama M and Shirakashi J I 2007 Control of tunnel resistance of nanogaps by field-emission-induced electromigration *Japan. J. Appl. Phys.* 2 **46** L907–9
[116] Shibata K, Buizert C, Oiwa A, Hirakawa K and Tarucha S 2007 Lateral electron tunneling through single self-assembled InAs quantum dots coupled to superconducting nanogap electrodes *Appl. Phys. Lett.* **91** 112102
[117] Araki K, Endo H, Tanaka H and Ogawa T 2004 Multi-curve fitting analysis of temperature-dependent I–V curves of poly-hexathienylphenanthroline-bridged nanogap electrodes *Japan. J. Appl. Phys.* 2 **43** L634–6
[118] Kronholz S, Karthauser S, van der Hart A, Wandlowski T and Waser R 2006 Metallic nanogaps with access windows for liquid based systems *Microelectron. J.* **37** 591–4
[119] Higuchi Y, Ohgami N, Akai-Kasaya M, Saito A, Aono M and Kuwahara Y 2006 Application of simple mechanical polishing to fabrication of nanogap flat electrodes *Japan. J. Appl. Phys.* 2 **45** L145–7
[120] Sedgwick T O, Broers A N and Agule B J 1972 A novel method for fabrication of ultrafine metal lines by electron beams *J. Electrochem. Soc.* **119** 1769–71
[121] Molzen W W, Broers A N, Cuomo J J, Harper J M E and Laibowitz R B 1979 Materials and techniques used in nanostructure fabrication *J. Vac. Sci. Technol.* **16** 269–72
[122] Goto T, Degawa K, Inokawa H, Furukawa K, Nakashima H, Sumitomo K, Aoki T and Torimitsu K 2006 Molecular-mediated single-electron devices operating at room temperature *Japan. J. Appl. Phys.* 1 **45** 4285–9
[123] Naitoh Y, Liang T T, Azehara H and Mizutani W 2005 Measuring molecular conductivities using single molecular-sized gap junctions fabricated without using electron beam lithography *Japan. J. Appl. Phys.* 2 **44** L472–4
[124] Kanda A, Wada M, Hamamoto Y and Ootuka Y 2005 Simple and controlled fabrication of nanoscale gaps using double-angle evaporation *Physica* E **29** 707–11
[125] Lefebvre J, Radosavlijević M and Johnson A T 2000 Fabricatin of nanometer size gaps in a metallic wire *Appl. Phys. Lett.* **76** 3828–30
[126] De Poortere E P, Stormer H L, Huang L M, Wind S J, O'Brien S, Huang M and Hone J 2006 1-to 2 nm-wide nanogaps fabricated with single-walled carbon nanotube shadow masks *J. Vac. Sci. Technol.* B **24** 3213–6
[127] De Poortere E P, Stormer H L, Huang L M, Wind S J, O'Brien S, Huang M and Hone J 2006 Single-walled carbon nanotubes as shadow masks for nanogap fabrication *Appl. Phys. Lett.* **88** 143124
[128] Chen Z, Hu W C, Guo J and Saito K 2004 Fabrication of nanoelectrodes based on controlled placement of carbon nanotubes using alternating-current electric field *J. Vac. Sci. Technol.* B **22** 776–80
[129] Chopra N, Xu W T, De Long L E and Hinds B J 2005 Incident angle dependence of nanogap size in suspended

carbon nanotube shadow lithography *Nanotechnology* **16** 133–6
[130] Shigeto K, Kawamura M, Kasumov A Y, Tsukagoshi K, Kono K and Aoyagi Y 2006 Reproducible formation of nanoscale-gap electrodes for single-molecule measurements by combination of FIB deposition and tunneling current detection *Microelectron. Eng.* **83** 1471–3
[131] Nagase T, Gamo K, Ueda R, Kubota T and Mashiko S 2006 Maskless fabrication of nanogap electrodes by using Ga-focused ion beam etching *J. Microlith. Microfab. Microsyst.* **5** 011006
[132] Huang L, Xu L, Zhang H Q and Gu N 2002 Fabrication of a nano-scale gap by selective chemical deposition *Chem. Commun.* 72–3
[133] Yasutake Y, Kono K, Kanehara M, Teranishi T, Buitelaar M R, Smith C G and Majima Y 2007 Simultaneous fabrication of nanogap gold electrodes by electroless gold plating using a common medical liquid *Appl. Phys. Lett.* **91** 203107
[134] Ah C S, Yun Y J, Lee J S, Park H J, Ha D H and Yun W S 2006 Fabrication of integrated nanogap electrodes by surface-catalyzed chemical deposition *Appl. Phys. Lett.* **88** 133116
[135] Li C Z, He H X and Tao N J 2000 Quantized tunneling current in the metallic nanogaps formed by electrodeposition and etching *Appl. Phys. Lett.* **77** 3995–7
[136] Kashimura Y, Nakashima H, Furukawa K and Torimitsu K 2003 Fabrication of nano-gap electrodes using electroplating technique *Thin Solid Films* **438** 317–21
[137] Narambuena C F, Del Popolo M G and Leiva E P M 2003 On the reasons for stepwise changes in the tunneling current across metallic nanogaps *Nano Lett.* **3** 1633–7
[138] He H X, Boussaad S, Xu B Q, Li C Z and Tao N J 2002 Electrochemical fabrication of atomically thin metallic wires and electrodes separated with molecular-scale gaps *J. Electroanal. Chem.* **522** 167–72
[139] Chen F, Qing Q, Ren L, Tong L M, Wu Z Y and Liu Z F 2007 Formation of nanogaps by nanoscale Cu electrodeposition and dissolution *Electrochim. Acta* **52** 4210–4
[140] Mészáros G, Kronholz S, Karthäuser S, Mayer D and Wandlowski T 2007 Electrochemical fabrication and characterization of nanocontacts and nm-sized gaps *Appl. Phys.* A **87** 569–75
[141] Hatzor A and Weiss P S 2001 Molecular rulers for scaling down nanostructures *Science* **291** 1019–20
[142] Anderson M E, Smith R K, Donhauser Z J, Hatzor A, Lewis P A, Tan L P, Horn M W and Weiss P S 2002 Exploiting intermolecular interactions and self-assembly for ultrahigh resolution nanolithography *J. Vac. Sci. Technol.* B **20** 2739–44
[143] Anderson M E, Tan L P, Tanaka H, Mihok M, Lee H, Horn M W and Weiss P S 2003 Advances in nanolithography using molecular rulers *J. Vac. Sci. Technol.* B **21** 3116–9
[144] Negishi R, Hasegawa T, Terabe K, Aono M, Tanaka H, Ogawa T and Ozawa H 2007 I–V characteristics of single electron tunneling from symmetric and asymmetric double-barrier tunneling junctions *Appl. Phys. Lett.* **90** 223112
[145] Negishi R, Hasegawa T, Terabe K, Aono M, Ebihara T, Tanaka H and Ogawa T 2006 Fabrication of nanoscale gaps using a combination of self-assembled molecular and electron beam lithographic techniques *Appl. Phys. Lett.* **88** 223111
[146] McCarty G S 2004 Molecular lithography for wafer-scale fabrication of molecular junctions *Nano Lett.* **4** 1391–4
[147] Liu S H, Tok J B H and Bao Z N 2005 Nanowire lithography: Fabricating controllable electrode gaps using Au–Ag–Au nanowires *Nano Lett.* **5** 1071–6
[148] Qin L, Jang J-W, Huang L and Mirkin C A 2007 Sub-5 nm gaps prepared by on-wire lithography: correlating gap size with electrical tansport *Small* **3** 86–90
[149] Chen C C, Sheu J T, Chiang S L and Sheu M L 2006 A novel nanofabrication technique for the array of nanogap electrodes *Japan. J. Appl. Phys.* 1 **45** 5531–4
[150] Tyagi P, Li D, Holmes S M and Hinds B J 2007 Molecular electrodes at the exposed edge of metal/insulator/metal trilayer structures *J. Am. Chem. Soc.* **129** 4929–38
[151] Luber S M, Zhang F, Lingitz S, Hansen A G, Scheliga F, Thorn-Csanyi E, Bichler M and Tornow M 2007 High-aspect-ratio nanogap electrodes for averaging molecular conductance measurements *Small* **3** 285–9
[152] Luber S M, Strobel S, Tranitz H-P, Wegscheider W, Schuh D and Tornow M 2005 Nanometre spaced electrodes on a cleaved AlGaAs surface *Nanotechnology* **16** 1182–5
[153] Dirk S M, Howell S W, Zmuda S, Childs K, Blain M, Simonson R J and Wheeler D R 2005 Novel one-dimensional nanogap created with standard optical lithography and evaporation procedures *Nanotechnology* **16** 1983–5
[154] Chen W, Liu X, Tan Z, Likharev K K, Lukens J E and Mayr A 2006 Fabrication and characterization of novel cross point structures for molecular electronic integrated circuits *J. Vac. Sci. Technol.* B **24** 3217–20
[155] Prokopuk N, Son K-A and Waltz C 2007 Electron tunneling through fluid solvents *J. Phys. Chem.* C **111** 65333–7
[156] Kushmerick J G, Lazorcik J, Patterson C H, Shashidhar R, Seferos D S and Bazan G C 2004 Vibronic contributions to charge transport across molecular junctions *Nano Lett.* **4** 639–42